OXFORD
SOT | Society of Toxicology
www.toxsci.oxfordjournals.org
ToxSci 20 Years

TOXICOLOGICAL SCIENCES, 161(2), 2018, 349–374

doi: 10.1093/toxsci/kfx221
Advance Access Publication Date: October 23, 2017
Research Article

2.45-GHz Microwave Radiation Impairs Hippocampal Learning and Spatial Memory: Involvement of Local Stress Mechanism-Induced Suppression of iGluR/ERK/CREB Signaling

Saba Shahin,* Somanshu Banerjee,* Vivek Swarup,† Surya Pal Singh,‡ and Chandra Mohini Chaturvedi*,[1]

*Molecular Neuroendocrinology Laboratory, Department of Zoology, Institute of Science, Banaras Hindu University, Varanasi, UP 221005, India; †Program in Neurogenetics, Department of Neurology, David Geffen School of Medicine, University of California, Los Angeles, California 90095; and ‡Department of Electronics Engineering, Indian Institute of Technology, Banaras Hindu University, Varanasi, UP 221005, India

[1]To whom correspondence should be addressed. Fax: 91 542 2368323; E-mail: cmchaturvedi@bhu.ac.in.

ABSTRACT

Microwave (MW) radiation induced oxidative stress reduces dendritic arborization, spine density and number of hippocampal pyramidal neurons and hence, impair learning and spatial memory through p53-dependent/independent apoptosis of hippocampal neuronal and nonneuronal cells. However, the mechanisms responsible for MW radiation induced impairment in memory formation remains still unknown. This study elucidates the effect of short (15 days) and long-term (30 and 60 days) low level 2.45 GHz MW radiation-induced local stress on the hippocampal spatial memory formation pathway in adult male mice. Twelve-weeks old mice were exposed to 2.45 GHz MW radiation (continuous-wave with overall average Power density of 0.0248 mW/cm^2 and overall average whole body SAR value of 0.0146 W/Kg) @ 2 h/d for 15, 30, and 60 days. Learning and spatial memory was assessed by 8-arm radial maze. We have investigated the alterations in serum corticosterone level and the expression of glucocorticoid receptor, corticotropin-releasing hormone (CRH), inducible nitric oxide synthase (i-NOS), iGluRs, PSD-95-neuronal NOS (n-NOS) system, protein kinase A, protein kinase Cε-ERK1/2-pERK1/2 in all the hippocampal subregions, viz. CA1, CA2, CA3, and DG through immunohistochemistry/immunofluorescence and alterations in the expression of hippocampal glucocorticoid receptor, CRH-receptor 1 (CRH-R1), cAMP-response element-binding (CREB), and phosphorylated-CREB (p-CREB) through western blot analysis. We observed that 2.45 GHz MW irradiated mice showed slow learning and significantly increased number of working and reference memory errors in radial maze task. Further, 2.45 GHz MW radiation exposure increases serum corticosterone level and the expression of CRH, CRH-R1, and i-NOS, while the expression of iGluRs, n-NOS, PSD-95, protein kinase Cε, protein kinase A, ERK-p-ERK, CREB, and p-CREB decreases in above mentioned hippocampal subregions in a duration dependent manner. Our findings led us to conclude that 2.45 GHz MW radiation exposure induced local stress suppresses signaling mechanism(s) of hippocampal memory formation.

Key words: microwave radiation; hippocampal stress; learning and memory formation; glutamate receptors; PSD-95; signaling molecules.

Microwave (MW) radiation is a type of nonionizing electromagnetic radiation (EMR). MWs, with a frequency range of 0.3–300 GHz and a wavelength of 1 mm to 1 m, are generated by the oscillation of electrically charged particles in an electromagnetic field in the free space. Studies from our and other laboratories have demonstrated MW radiation as one of the strongest environmental stressor, responsible for inducing oxidative/nitrosative stress by havoc generation of free radicals (reactive oxygen [ROS]/nitrogen species [RNS]) (Shahin *et al.*, 2013, 2014, 2015; Yakymenko *et al.*, 2016). Among all the body organs, brain is highly vulnerable to free radical attacks and subsequently undergoes lipid peroxidation (LPO) (Butterfield *et al.*, 2002) due to high content of polyunsaturated fatty acids. Any imbalance in ROS/RNS homeostasis can lead to neuronal damage/neurodegeneration (Bressler *et al.*, 2007), altered excitatory glutamatergic synaptic transmission, long-term potentiation (LTP) and synaptic plasticity, which altogether result into cognitive/memory impairments (Gispen and Biessels, 2000).

Memory processes, which involves hippocampal circuitry (Eichenbaum *et al.*, 2007), at the physiological/cellular level, are mediated through the involvement of LTP formation and stabilization of synaptic functions (Neves *et al.*, 2008). Both short term and chronic stress has been shown to effect memory formation and influences hippocampal structure and function (Joëls and Baram, 2009). Previous studies have shown that MW radiation induced stress can affect learning and memory (Wang and Lai, 2000; Shahin *et al.*, 2015). Exposure to continuous-wave (CW) as well as pulse field 2.45 GHz MW radiation results in cognitive malfunction and spatial memory deficits (Lai *et al.*, 1994; Wang and Lai, 2000). In contrary, Cassel and other groups reported that exposure to 2.45 GHz MW radiation does not affect/alter the radial arm maze (RAM) performance as well as learning and memory (Cassel *et al.*, 2004; Cosquer *et al.*, 2005).

In response to different stressors as well as acute and/or chronic stress, hypothalamic corticotropin-releasing hormone (CRH) neurons in paraventricular nucleus become activated and eventually stimulate the adrenals to release Glucocorticoids (GCs). The excessive GC secretion can damage the structural integrity of neurons and may result in dendritic atrophy in the hippocampus (McEwen, 2000; Vyas *et al.*, 2002) and attenuated LTP (Pavlides *et al.*, 2002). Glucocorticoid receptor (GR), expressed throughout the brain, is the dominant receptor that mediates effects of stress levels of GCs, and helps to maintain GC levels within specific limits (Kretz *et al.*, 1999). GR-induced neuritic/dendritic atrophy and neuronal death is also linked with mood disorders and cognition as well as neuroendocrine dysregulation (McEwen, 2000; Sousa and Almeida, 2002).

Chronic stress has been shown to alter protein levels of PSD-95 (Cohen *et al.*, 2011), neuronal nitric oxide synthase (n-NOS) (Gadek-Michalska *et al.*, 2015) and ionotropic glutamate receptors (iGluRs: AMPA and NMDA: directly associated with ligand-gated ionophores permitting Ca^{2+} influx) in the mouse brain (Kallarackal *et al.*, 2013). iGluR-mediated activation of postsynaptic PSD-95-nNOS is required for the development of the excitatory postsynaptic currents which subsequently activate the downstream kinases. ERK/MAPK/MEK or ERK-mediated cAMP-response element-binding (CREB) signaling pathway plays a pivotal role in LTP formation and memory storage as protein template in the dendritic spines (Kelleher *et al.*, 2004). The cross-talks and interactions of different downstream kinases and phosphatases are essential for the hippocampal dependent learning (Cammarota *et al.*, 2005) and spatial memory formation (Adams and Sweatt, 2002). Glutamate release in the synaptic cleft activates the AMPA receptors at the post synaptic density. Activated AMPA and NMDA receptors cause increased intracellular Ca^{2+} level thereby activating protein kinase C (PKC) and protein kinase A (PKA) (Lynch, 2004). PKC, PKA, and CaMKIIα further induce ERK activation that leads to phosphorylation of the CREB protein which is a key element in consolidation of memory (Choe and Wang, 2001). Thus, ERK may participate in learning and memory formation mediated by activated iGluRs, as crosstalk exists among ERK, PKC, and PKA (Adams and Sweatt, 2002).

In our previous study, we have already demonstrated that 2.45 GHz MW radiation induced oxidative and nitrosative stress in hippocampus impairs the learning and spatial memory by causing apoptosis of neuronal and nonneuronal cells (Shahin *et al.*, 2015). MW radiation-induced stress also showed reduced dendritic arborization, branching, spine density as well as shortening of dendritic processes, neuronal/dendritic atrophy, and neuronal clumping and hence, results in learning and spatial memory deficits (Shahin *et al.*, 2015). However, the mechanisms responsible for MW radiation induced learning and memory impairment is still unknown. Hence this study was undertaken to elucidate the effect of short (15 days) and long-term (30 and 60 days) low level 2.45 GHz MW CW radiation-induced stress on the classical hippocampal memory formation pathway and resultant alterations in hippocampal learning and memory processes.

Hippocampal loss of synapse-bearing dendrites and dendritic spines is closely associated with memory deficits. Now, to look into the deeper insights of mechanisms behind the learning and spatial memory impairment following 2.45 GHz MW radiation, we hypothesized that MW radiation-induced oxidative and nitrosative stress may trigger the stress responses through the corticosterone-hippocampal GR and hippocampal CRH-CRH-receptor 1(CRH-R1) pathways. The 2.45 GHz MW radiation induced free radical load may also suppress iGluRs (AMPA and NMDA receptor subtypes) at the glutamatergic synapse and hence, may inhibit the downstream PSD-95-nNOS signaling and downstream memory forming kinases (PKA-PKC-ERK1/2 and phosphorylated-ERK1/2), that are essential for the LTP/long-term memory (LTM) formation and stabilization.

Hence we investigated the alterations in (1) learning and spatial memory, (2) corticosterone level, (3) expression of GR, CRH-CRHR1, (4) iGluRs (AMPA and NMDA receptor subtypes), (5) downstream signaling molecules involved in the memory formation pathway (PSD-95-nNOS-inducible NOS (i-NOS) system, PKA-PKCε-ERK1/2 and phosphorylated ERK1/2 and CREB and phosphorylated-CREB (p-CREB) in all the hippocampal subregions, viz. CA1, CA2, CA3, and DG.

MATERIALS AND METHODS

Animals. Twelve-week-old Swiss strain male mice (body weight approximately 30 g) were obtained from the mice colony of our laboratory maintained in a controlled environment with 12-h light:dark cycle (LD12:12) and 24°C ± 2°C room temperature. Animals were kept under steady-state, received standard commercial pelleted food and water *ad libitum*. Four animals per cage were housed in standard ventilated polypropylene cages with dry husk as the bedding material. Animals were treated and animal protocols were performed humanely and with regard to alleviation of suffering. All the experimental procedures were approved and performed as per the guidelines of "Institutional Animal Ethical Committee, Institute of Science, Banaras Hindu University" and within the framework of the revised animals (Scientific procedures) act of 2002 of the

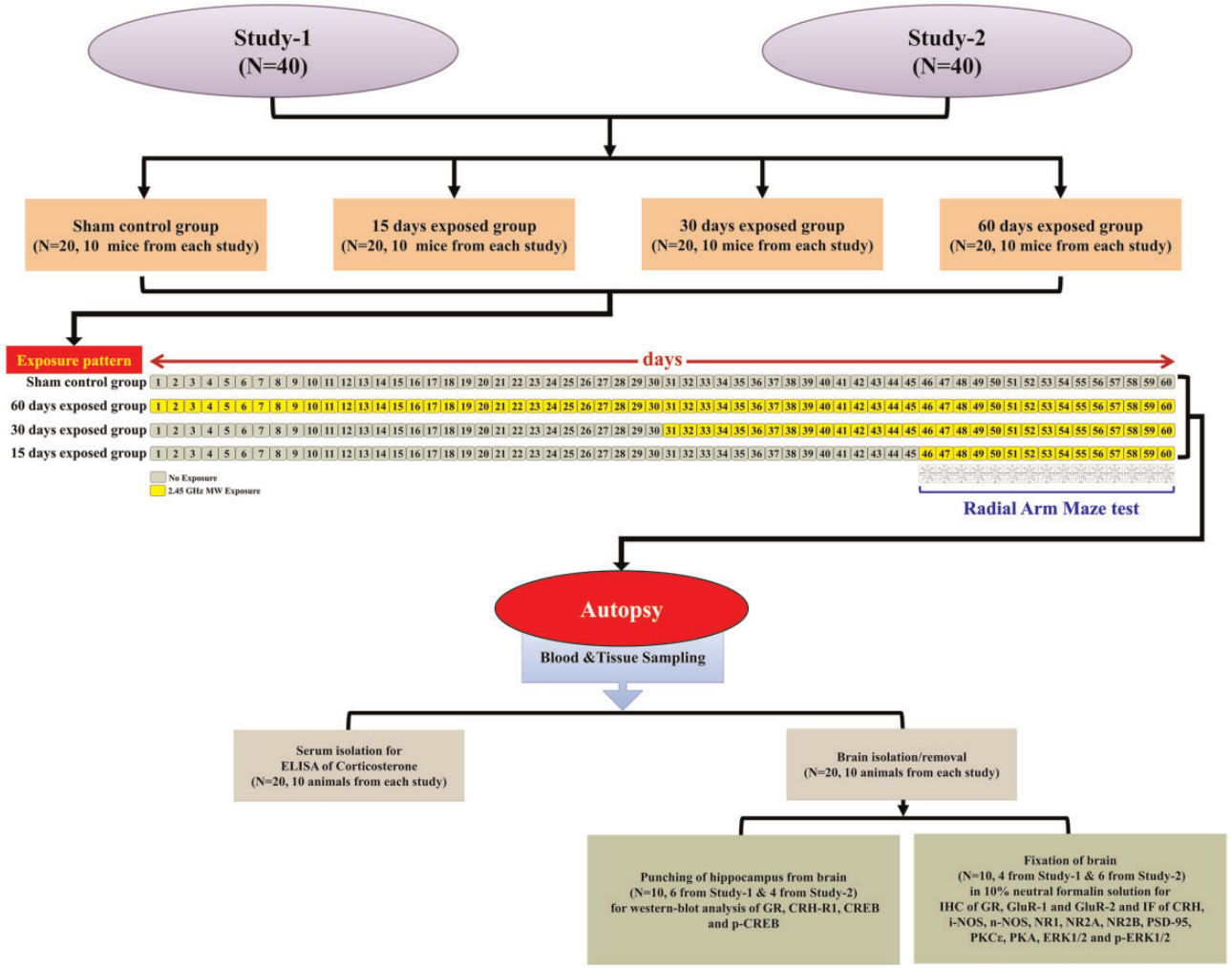

Figure 1. Schematic representation of experimental design to study the time/duration dependent effect of 2.45 GHz MW radiation on learning and memory formation pathway.

Government of India on Animal welfare. ARRIVE guidelines were followed to report this study.

Study design. Forty (40) randomly selected mice were divided into 4 groups (1 sham control and 3 experimental ie, 15 days exposed; 30 days exposed and 60 days exposed group) of 10 mice each ($n = 10$). The 3 experimental group mice were exposed to 2.45 GHz (CW) MW radiation for 2 h/d from 09:00 h to 11:00 (30 days), 11:30 to 13:30 h (60 days) and 14:00–16:00 h (15 days) continuously. The control group mice were subjected to sham exposure for 60 days [only 1 sham control of maximum duration ie, 60 days sham exposed group was taken into account to nullify the cage related and other external constraints]. Rectal temperature of all the mice was monitored during the first and the last 3 days of exposure.

Experiment was repeated hence the data presented is from total 20 animals per group including RAM test and corticosterone assay. Further, out of total 20 animals in each group, 10 animals (4 from study-1 and 6 from study-2) used for immunohistochemistry and immunofluorescence and rest 10 animals (6 from study-1 and 4 from study-2) were processed for western blot (Figure 1).

MW exposure. Experimental mice were exposed to 2.45 GHz MW radiation by using MW irradiation set-up facility as describe previously (Shahin *et al.*, 2015) at overall average Power density of 0.0248 mW/cm^2 and overall average specific absorption rate (SAR) value of 0.0146 W/Kg. The SAR value was estimated for body length parallel to the electric field, as per actual placement of the mouse (Gandhi *et al.*, 1977; Shahin *et al.*, 2013, 2014). The detailed description of MW generator, animal cage designed for MW exposure, Power density, and SAR value calculation has been already mentioned in our previous study (Shahin *et al.*, 2015). The exposure at overall average Power density of 0.0248 mW/cm^2 did not cause any elevation in the ambient temperature of animal cage as well as mice rectal temperature. The average observed rectal temperature of the mice were 35.81°C ± 0.2 °C (control group) and 35.9°C ± 0.2 °C (experimental group) during first 3 days of exposure and 35.91°C ± 0.2 °C (control group) and 35.95°C ± 0.2 °C (experimental group) after the end of exposure.

RAM test. To analyze the learning and spatial memory, 8-RAM test was performed according to the protocol of Albayram *et al.* (2012) as described previously. Briefly, the 8-RAM apparatus

consisted of a central platform of diameter 25 cm and 8 identical arms of 70 cm (length) × 10 cm (width) × 15 cm (height) each. These arms extend radially from a central platform at an equal angle. The whole RAM apparatus was placed at a fixed position. A reward of food was kept at the end of each arm. To access the spatial memory, 4 alternate arms were baited throughout the experiment. The test was performed in 3 phases: (1) habituation phase, which continued for 2 days of exploratory trials (10 min) to prepare the animals for the maze; (2) training phase, which consisted 2 consecutive trials (5 min each) performed once a day for 12 consecutive days and (3) Probe test phase, which consisted 1 trial of 5 min. Probe test was performed 24 h after the last training day ie, after the end of last day of exposure. During habituation, all the 8 arms were baited with food reward (chocolate-flavored food pellets) while during training phase, 4 randomly selected alternate arms were baited. Probe test was performed on un-baited (ie, arms with no food reward) 8 arms maze to assess the LTM. Entry into arm was counted when all 4 paws of the animal crossed the entrance of the arm. The first entry into the previously nonbaited arms was considered as reference memory error (RME) and re-entry in a previously visited baited arm was considered as working memory error (WME). For RME and WME, bar graphs were plotted for 12 days of training phase. Memory consolidation was assessed by calculating the % time spent in previously baited arms and performance rate as described previously in Nikbakht *et al.* (2012) by using the formula,

$$P = \frac{n - (\mathrm{RME} + \mathrm{WME})}{N} \times 100$$

where n refers to the total number of arm entries made in the trial. RAM test was performed under blind condition during the last 15 days of exposure. After the completion of each exposure, animals were transferred to laboratory cages and handed over to an experimenter (who did not know the exposure conditions) to perform the RAM test.

Blood collection and tissues sampling. Twenty-four hour after the last day of MW exposure, mice were sacrificed by decapitation. Blood was collected in nonheparinized tubes for serum collection. Brain was dissected out. Hippocampus was separated through punching from the brain of 10 mice (n = 10, 6 from study-1 and 4 from study-2) and stored at −20 °C after washing with ice-cold sterile physiological saline until processed for western-blot analysis of GR, CRH-R1, CREB, and p-CREB. Brain of other 10 mice (n = 10, 4 from study-1 and 6 from study-2) from each group was fixed in 10% neutral formalin solution for immunohistochemistry and immunofluorescence.

Serum isolation and ELISA of corticosterone. Blood samples were kept at room temperature for 30 min and then centrifuged at 4000 rpm at 4 °C for 15 min. The supernatant was collected as serum and used for corticosterone estimation. For serum corticosterone levels, an enzyme immunoassay was performed using a commercial DRG Corticosterone enzyme immunoassay Kit (DRG Corticosterone [Rat/Mouse] Elisa [EIA-5186], IBL International GmbH, Hamburg, Germany) following the manufacturer's protocol. The antiserum used in the assay was specific for corticosterone. The cross-reactivity of the assay was 100% with corticosterone, 0.2% with Aldosterone, 0.3% with cortisol, 2.4% with 11-Deoxycorticosterone, 0.7% with progesterone, but cross-reactivity with dehydroepiandrosterone, estriol, estradiol, 17-hydroxyprogesterone, testosterone, 18-hydroxydeoxycorticosterone, pregnolone is not detectable. The analytical sensitivity of the assay was 4.1 ng ml^{-1}. The intra-assay coefficient of variation (CV) was 2.8%–8.3% whereas the inter-assay CV was 4.8%–12.4%.

Tissue homogenization. 10% (w/v) homogenate of hippocampus was prepared for both control and experimental groups in a protein extraction buffer containing 50 mM Tris–HCl (pH 7.6), 0.25 M sucrose, 150 mM NaCl, 1 mM EDTA (pH 7.4), 1% Triton X-100, 0.5% sodium deoxycholate, leupeptin (1 μg/ml) aprotinine (2 μg/ml) and phenylmethylsulfonyl fluoride (100 μg/ml) (PMSF), 10 mM DTT, using a Polytron homogenizer and kept on ice for 20 min. After centrifugation at 12 000 rpm for 25 min at 4 °C, supernatant was collected. Total protein concentration was measured by Bradford's method using bovine serum albumin (BSA) as the standard (Bradford, 1976).

SDS-PAGE and western blot analysis. Equal amount of protein (50 μg) from each group was resolved on 8%–12% SDS–polyacrylamide gel (SDS–PAGE) at constant setting of 50 V for 30 min and then at 100 V for 1 h, using the Mini-PROTEAN tetra system, BIO-RAD, USA. The resolved proteins were transferred from the polyacrylamide gel to PVDF membrane (Millipore, USA) by electro-blotting for 15–18 min in a Semidry blotting apparatus (TRANS-BLOT SD, Semidry transfer cell, BIO-RAD) at constant setting of 15 V. Membranes were then blocked by either 5% fat free skimmed (dry) milk in Tris buffered saline with 0.1% Tween-20 (TBST) or 5% (BSA for p-CREB) for 2 h at room temperature. The membranes were then incubated overnight (for 16–20 h) in primary antibodies (against the different antigens with standardized specific dilutions-enlisted in Table 1) for the quantitative analysis of variation in the expression level of the antigens including β-actin, in 1%–2.5% milk TBST or 2.5% BSA (for p-CREB). Membranes were washed (3–5 min) and incubated with secondary antibody (antirabbit/antimouse IgG-HRP conjugate, diluted 1:4000, respectively) for 2 h and then washed (2 washes for 15 min each) with TBST. Immunoreactive proteins were visualized by using Super Signal West Pico Chemiluminescent Substrate, Thermo Scientific, USA; Catalog number: 34080. NEXGEN-Clear BLUE Pre-stained Protein Ladder (Cat. No. PG700-0500PI) were used as standard Prestained molecular weight markers. Experiment was repeated thrice with the same result and single representative blot was provided. Equal loading was confirmed with β-actin. The same membranes of primaries were stripped and re-probed with antiβ-actin antibody to normalize for protein loading.

The intensity of the bands was quantitated by gel densitometry using Image J software (Image J 1.48 bundled with 64-bit Java, NIH, USA). Using the software's tool, integrated density of all the bands was measured. To get the integrated relative density value (IRDV), the integrated density value of each protein band was determined and normalized levels of antigens were calculated by dividing the IDV of a protein band by the IDV of the β-actin.

Immunohistochemistry of GR and GluRs. Immunohistochemistry for GR, GluR-1, and GluR-2 were carried out on neutral formalin-fixed paraffin-embedded brain sections using monoclonal (GR) and polyclonal (GluR-1 and GluR-2) antibodies. Immunohistochemistry was performed in a 2-step procedure by using Vectastain ABC kit (Vector Laboratories, Burlingame, California). In the first step, after initial deparafinization in xylene and rehydration in a graded series of alcohol, antigen retrieval was performed using 1 mol l^{-1} citrate buffer (pH 6) in a

Table 1. Details of the Antibodies Used in This Study

Antibodies	Source/Gifted by	Dilution (IHC)	Dilution (IF)	Dilution (WB)
CRH (PFU-83) (rat monoclonal)	Dr Anne-Marie van Dam, Amsterdam, Netherlands	—	1:1000	—
CRH-R1 (rabbit polyclonal)	Cat. No: 720290, Thermo fisher Scientific, USA	—	—	1:2000
GR (mouse monoclonal)	Dr Jack E. Bodwell, Dartmouth, USA	1:1000	—	1:3000
i-NOS (N-20) (rabbit polyclonal)	sc-651, Santa Cruz Biotechnology, USA	—	1:50	—
GluR-1 (rabbit polyclonal)	Prof. Richard L. Huganir, Baltimore, USA	1:500	—	—
GluR-2 (rabbit polyclonal)				
NR1 (N308/48) (mouse monoclonal)	UC Davis/NIH NeuroMab Facility,	—	1:100	—
NR2A (N327/95) (mouse monoclonal)	UC Davis, Davis CA, USA			
NR2B (N59/20) (mouse monoclonal)				
PSD-95 (K28/43) (mouse monoclonal)				
n-NOS (goat polyclonal)	ab1376, Abcam, Cambridge, USA	—	1:100	—
PKCε (C-15) (rabbit polyclonal)	sc-214, Santa Cruz Biotechnology, USA	—	1:50	—
PKAα (A-2) (mouse monoclo nal)	sc-28315, Santa Cruz Biotechnology, USA	—	1:50	—
ERK1/2(H-72) (rabbit polyclonal)	sc-292838, Santa Cruz Biotechnology, USA	—	1:50	—
p-ERK1/2 (12D4) (mouse monoclonal)	sc-81492, Santa Cruz Biotechnology, USA	—	1:50	—
CREB (86B10) (mouse polyclonal)	CST No. 9104, Cell Signaling Technology, USA	—	—	1:250
p-CREB (Ser133) (87G3) (rabbit monoclonal)	CST No. 9198, Cell Signaling Technology, USA	—	—	1:250
β-actin (mouse monoclonal)	A00702-40 Genscript, USA	—	—	1:2500

MW oven at 1000 W (3–4 min). Tissue sections were then treated with blocking solution (5% heat-inactivated goat serum) for 2 h at room temperature and then tissue sections of brain were incubated with mouse-GR antibody (1:1000), rabbit-GluR-1 antisera (1:500) and rabbit-GluR-2 antisera (1:500) with specificity to the corresponding antigen of interest, for 24 h in a humid chamber. The second step was incubation of the sections with biotinylated Universal (antimouse IgG/rabbit IgG) antibody [PK-6200-VECTASTAIN Elite ABC HRP Kit (Peroxidase, Universal)] for 2 h in room temperature and were washed repeatedly (3–4 times washing, each of 5 min). The sections were then incubated with ABC reagent conjugated with horseradish peroxidase (HRP) (PK-6200) for 30 min. Finally, DAB (diaminobenzidine hydrochloride-SIGMA FAST DAB with metal enhancer, Cat. No. D0426, Sigma-Aldrich, St Louis, Missouri) with nickel chloride solution, a component of DAB Substrate Kit (SK-4100), was used as a chromogen molecule for the immunological detection. Thereafter, sections were dehydrated through an ascending ethanol series, cleared in xylene and then mounted using DPX. The sections were viewed under a microscope (Axioskop 2 Plus; Carl Zeiss, Oberkochen, Germany). Images were captured at the same magnification with an Axioskop HRcam camera and stored as TIFF files for immunohistochemistry signal analysis.

Immunofluorescence and confocal microscopy. Immunofluorescence of CRH, i-NOS, n-NOS, NR1, NR2A, NR2B, PSD-95, PKCε, PKA, ERK1/2, and p-ERK1/2 in brain sections was performed. Immunofluorescence was performed in a 2-step procedure as described by Banerjee *et al.* (2016). Briefly, in the first step, tissue section slides were processed for initial deparafinization in xylene and rehydration in graded series of alcohol. Antigen retrieval was performed using 1 M citrate buffer (pH 6) in a MW oven at 1000 W (3–4 min). Tissue sections were then treated with blocking solution for 2 h at room temperature (5% Heat Inactivated Goat Serum) and the sections were then incubated with respecs. Coverslips were applied and then sealed with nail polish after ensuring the spread of the mounting medium over all the sections without any bubble formation). A Zeiss LSM510 Meta laser-scanning confocal microscope with a C-Apochr 40×, 1.2-NA, oil immersion objective was used to observe the sections, and the images were collected at the same magnification and stored as TIFF files using LSM 510 Meta software.

Image analysis. The variations in the degree of expression for all the above mentioned antigens in the hippocampal subregions (ie, DG, CA1, CA2, and CA3) of brain sections were determined by measuring the integrated optical density (IOD). Image analysis was performed as described elsewhere (Banerjee *et al.*, 2016). Briefly, for IOD measurement, the stored TIFF file images (of same magnification for all the above mentioned antigens in the hippocampal subregions [ie, DG, CA1, CA2, and CA3]) were imported to Image J software (Image J 1.48 bundled with 64-bit Java, National Institutes of Health, Bethesda, USA) and processed for analysis. Using the software's tool, IOD values of all the areas showing positive signals in different subregions of hippocampus were measured after normalizing to the background. The IOD values (relative units) were averaged (4 sections per brain and 10 brain per group) to determine signal density. Average IOD values of brain sections from each group were considered as arbitrary unit (a.u.) thresholds for each antigen (Supplementary Table 2). The processing and analysis were consistent between images. Statistics were performed on the average a.u. values (means ± SEM). On the basis of the difference in the level of significance (p value $< .05$), the IOD values were classified as intense, moderate or weak. Image analysis was performed blindly and separately by 2 observers.

Statistical analysis. All the data for behavioral test, corticosterone assay, western blot analysis, IHC and IF plates are presented as means ± SEM. The normality distribution for each type of dataset was assessed and verified using the Shapiro-Wilk test and also visually confirmed using Q-Q plot. RAM data were analyzed using 1-way repeated measures ANOVA with Bonferroni's *post hoc*. For corticosterone assay, western blot analysis and IOD values of IHC/IF plates, statistical analysis were performed by independent *t* test and 1-way ANOVA coupled with a Dunnet T3 *post hoc* analysis to determine the significance among the 4 different groups. A multiple comparison corrected p-value of $< .05$ was considered significant. Data were analyzed by using the statistical software package statistical analysis system (SPSS Statistics 17.0, IBM, Armonk, New York).

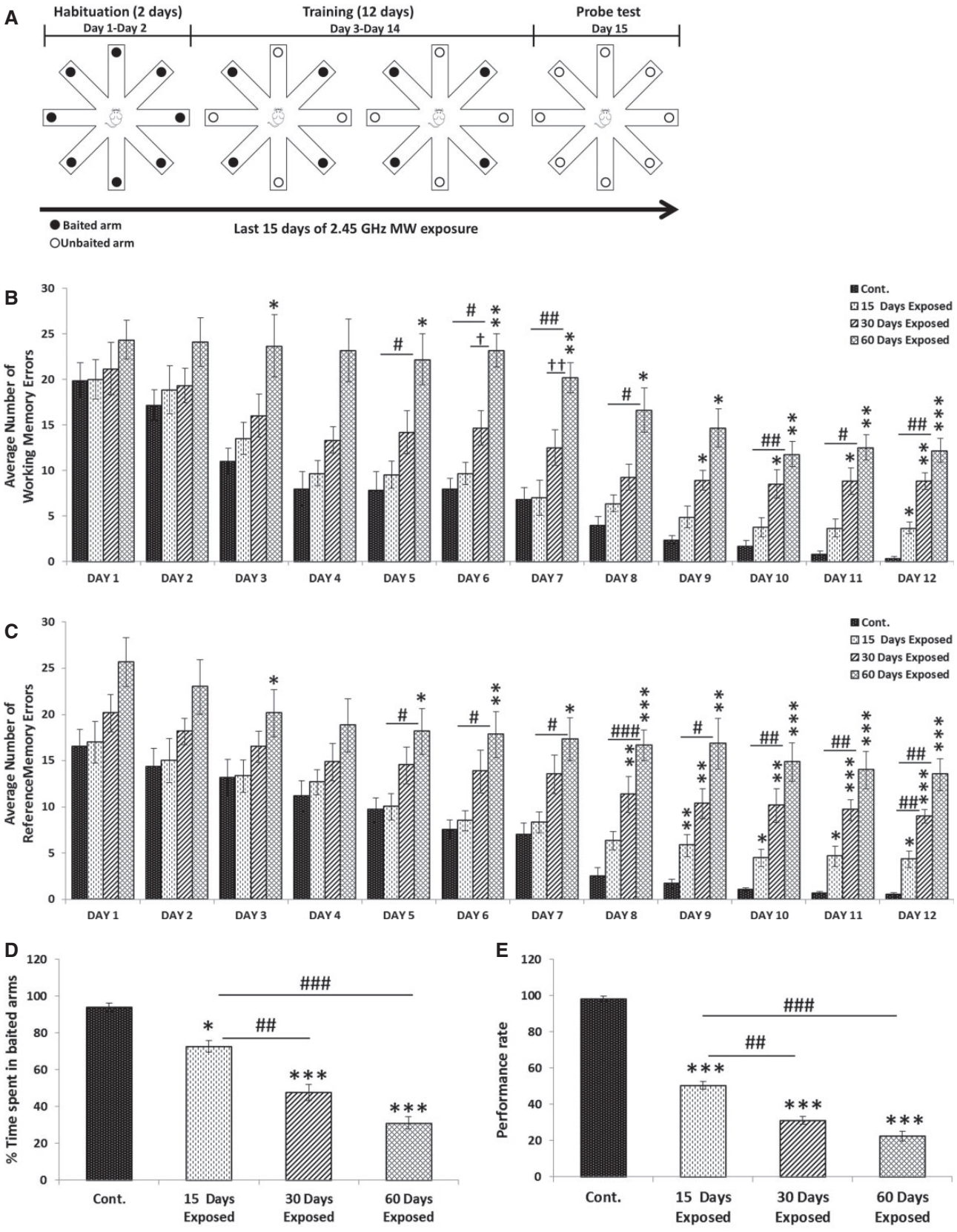

Figure 2. Duration dependent impact of 2.45 GHz MW radiation on learning and spatial memory impairment in exposed mice. A, Experimental design: Mice were habituated for 2 days and trained on 8-RAM for 12 days to evaluate learning and memory consolidation. Probe test was performed on 15th day ie, last day of exposure for all the groups. For probe test, mice were allowed to explore on the unbaited RAM. B, WMEs, (C) RMEs, (D) %Time spent in baited arms during the day of Probe trial and (E) Performance rate. Values are expressed as mean ± SEM (n = 20). $^{*}p < .05$, $^{**}p < .01$, $^{***}p < .001$ significance of difference from control; $^{\#}p < .05$, $^{\#\#}p < .01$, $^{\#\#\#}p < .001$ significance of difference from 15 days exposed group; $^{\dagger}p < .05$ significance of difference from 30 days exposed group.

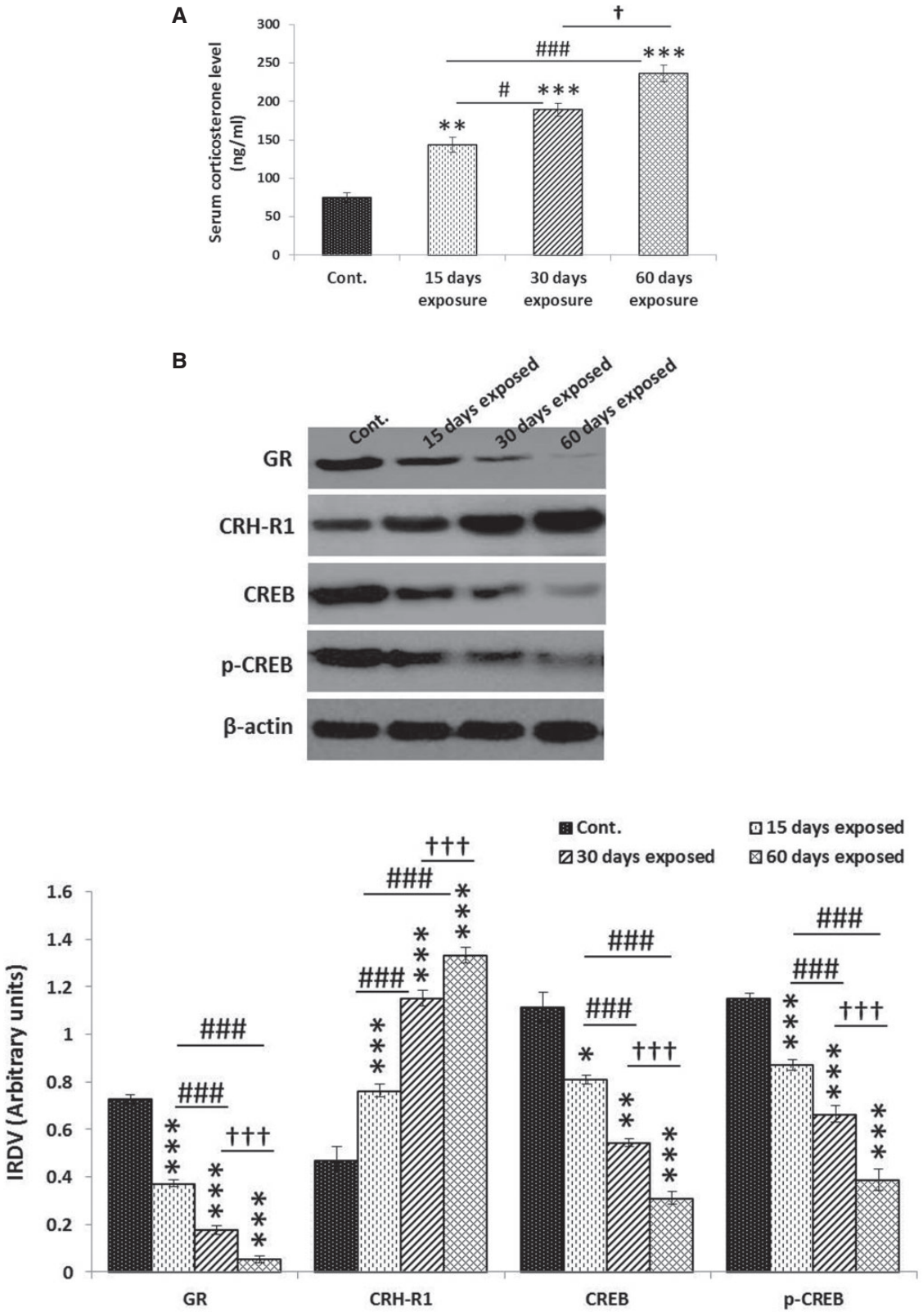

Figure 3. (A) Effect of CW 2.45 GHz MW radiation on serum corticosterone concentration in mice: Data are presented as mean ± SEM (n = 20). $^{**}p < .01$, $^{***}p < .001$ significance of difference from control; $^{\#}p < .05$, $^{\#\#\#}p < .001$ significance of difference from 15 days exposed group; $^{\dagger}p < .05$ significance of difference from 30 days exposed group. B, Western blot analysis of GR, CRH-R1, CREB protein, and p-CREB in the hippocampus of 2.45 GHz MW exposed groups. IRDV, integrated relative density value. Values are expressed as mean ± SEM (n = 10). $^{*}p < .05$, $^{**}p < .01$, $^{***}p < .001$ significance of difference from control; $^{\#\#\#}p < .001$ significance of difference from 15 days exposed group; $^{\dagger\dagger\dagger}p < .001$ significance of difference from 30 days exposed group.

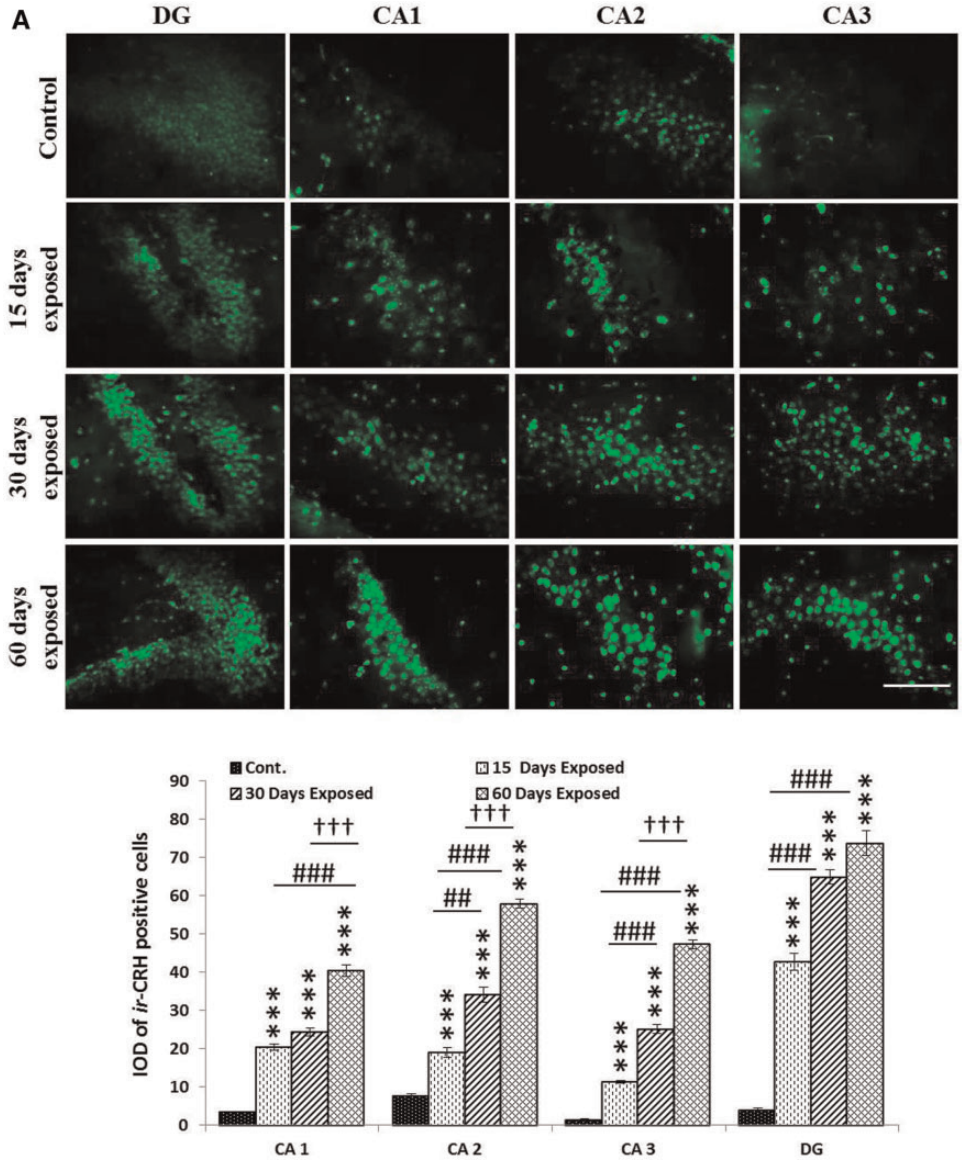

Figure 4. Immunofluorescence (CRH, i-NOS), immunohistochemistry (GR) and the IOD of (A) CRH, (B) GR and (C) i-NOS in CA1, CA2, CA3, and DG regions of hippocampus of mice exposed to 2.45 GHz MW radiation for different duration: When compared with control which shows weak immunoreactivity for CRH and i-NOS in few cells only, 15 days exposed group shows moderately increased immunoreactivity while 30 and 60 days exposed group shows strong and intense immunoreactivity in large/more number of cells. On the other hand, in control group very strong/intense immunoreactivity for GR was observed in CA1, CA2, CA3, and DG regions of hippocampus. 15 days exposed group shows moderate immunoreactivity while 30 and 60 days exposed group shows decreased immunoreactivity for GR compared with their respective controls. Scale bar = 50 μm. Values are expressed as mean ± SEM (n = 10). $^{***}p < .001$ significance of difference from control; $^{\#\#}p < .01$, $^{\#\#\#}p < .001$ significance of difference from 15 days exposed group; $^{\dagger}p < .05$, $^{\dagger\dagger}p < .01$, $^{\dagger\dagger\dagger}p < .001$ significance of difference from 30 days exposed group.

RESULTS

RAM Test

To assess learning and spatial memory 8-RAM test was performed (Figure 2A). In RAM task, 2.45 GHz MW irradiated mice showed slow learning than control during the training phase. They made more errors in recalling the baited arms (Figs. 2B and 2C). Significantly increased number of working memory (15 days exposed group: day 12, $p < .05$; 30 days exposed group: days 9–11, $p < .05$; day 12, $p < .01$; 60 days exposed group: days 3, 5, 8, and 9, $p < .05$; days 6, 7, 10, and 11, $p < .01$; day 12, $p < .001$, Figure 2B) and reference memory (15 days exposed group: day 9, $p < .01$; days 10–12, $p < .05$; 30 days exposed group: days 8–10, $p < .01$; days 11 and 12, $p < .001$; 60 days exposed group: days 3, 5, 7, $p < .05$, days 6 and 9, $p < .01$; days 8, 10–12, $p < .001$; Figure 2C) errors was made by 2.45 GHz MW radiation exposed mice during training phase compared with control. Further, the % time spent in previously baited arms (15 days exposed group, $p < .05$; 30 days exposed group, $p < .001$; 60 days exposed group, $p < .001$; Figure 2D) as well as the performance rate (15, 30, and 60 days exposed group, $p < .001$; Figure 2E) of all the MW radiation exposed group also decline significantly as compared with control. The decline in spatial memory and performance rate after 24 h of training indicates the impairment of memory consolidation due to MW radiation exposure. The degree of decrease in learning and spatial memory was more in

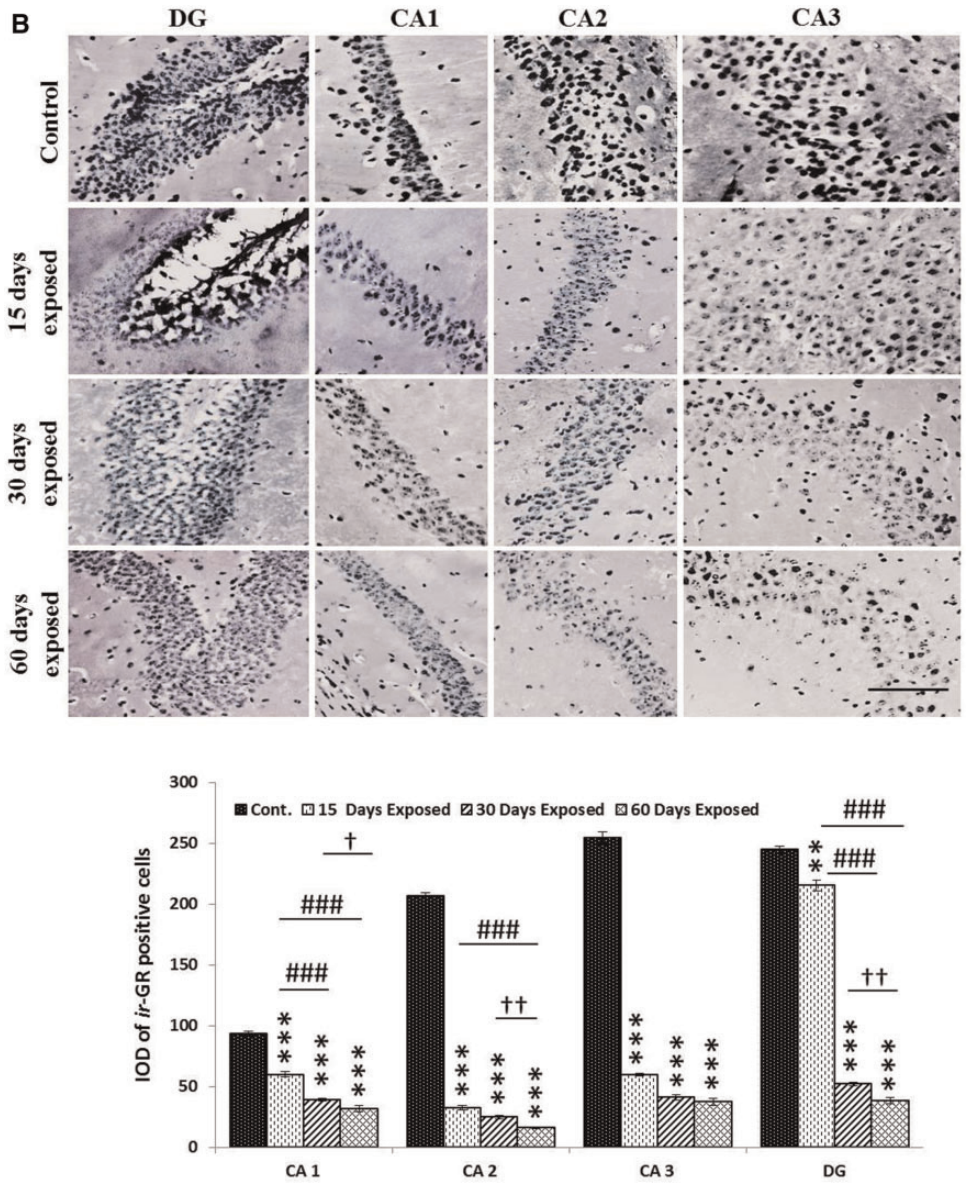

Figure 4. Continued

30 and 60 days of exposed group compared with 15 days exposed group.

CW 2.45 GHz MW Irradiation Induces Serum Corticosterone Level and Alters the Expression of CRH, CRH-R1, GR, and i-NOS in the Hippocampus of Mice

Brain tissue is highly vulnerable to MW irradiation induced stress; therefore, we first checked the level of serum corticosterone in different experimental groups. Serum corticosterone level was found to increase significantly in a duration-dependent manner in all the 2.45 GHz MW irradiated groups (15 days exposed group, $p < .01$; 30 and 60 days exposed group, $p < .001$) compared with control (Figure 3A).

Exposure to stress not only causes the fundamental changes in the state of the brain but may also leads to neurological disorders. As stress-induced neuronal cell death has been implicated in various neurological disorders and MW radiation is acting as a strong environmental stressor, therefore we checked the expression of CRH, CRH-R1, GR, and i-NOS in different hippocampal regions. We observed significant changes in the expression of CRH, CRH-R1, GR, and i-NOS in all the 2.45 GHz MW irradiated groups compared with control in duration dependent manner. Using immunofluorescence, we found that CRH immunoreactivity was very weak in control group in DG, CA1, CA2, and CA3 regions of hippocampus (Figure 4A). Strikingly, exposure to MW irradiation for 15 days showed significant increase in CRH immunoreactivity (DG: 11.21-fold increase, CA1: 5.98-fold increase, CA2: 2.50-fold increase, CA3: 7.88-fold increase; $p < .001$) which was further increased upon exposure to MW irradiation for 30 days (DG: 17.04-fold increase, CA1: 7.15-fold increase, CA2: 4.48-fold increase, CA3: 17.48-fold increase; $p < .001$) and 60 days (DG: 19.38-fold increase, CA1: 11.86-fold increase, CA2: 7.62-fold increase, CA3: 32.91-fold increase; $p < .001$) in all hippocampal regions compared with control. To gain further insights into the mechanism of CRH induction upon MW irradiation, we checked the protein expression levels of

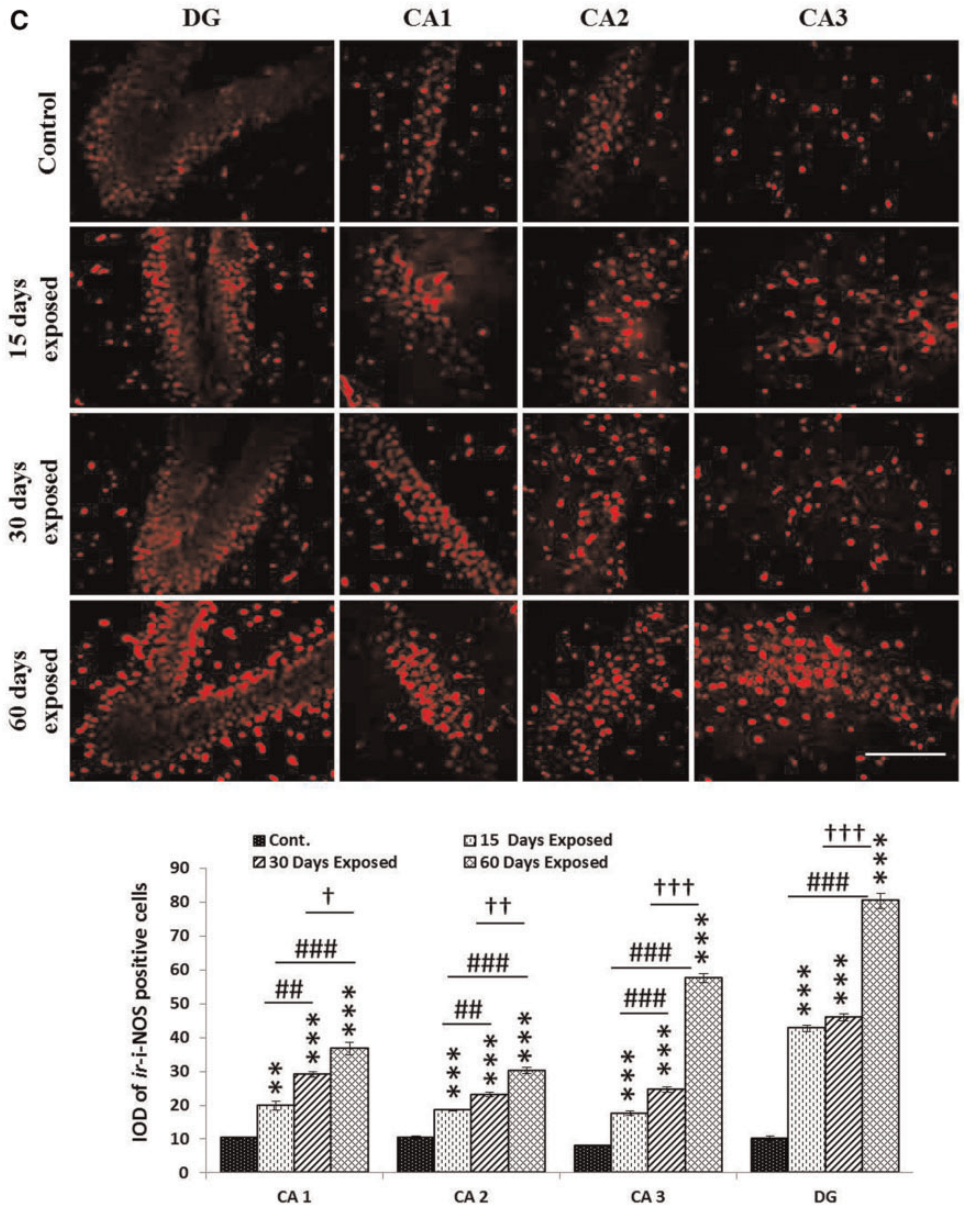

Figure 4. Continued

CRH receptor (CRH-R1), a G-protein coupled receptor, using western blot in hippocampal brain lysates. CRH-R1 binds CRH neuropeptide and regulates the hypothalamic-pituitary-adrenal (HPA) pathway. We found that the expression of CRH-R1 was significantly increased in the hippocampus of all the MW exposed groups (15, 30, and 60 days exposed groups, $p < .001$) compared with control (Figure 3B), indicating activation of CRH-CRH-R1 signaling.

In contrast to CRH-CRH-R1 activation, the immunoreactivity of GR decreased significantly in all the 2.45 GHz MW irradiated group compared with control (Figure 4B). Although the control group revealed strong/intense immunoreactivity for GR in DG, CA1, CA2, and CA3 regions of hippocampus, the GR immunoreactivity decreased in 15 days exposed group (DG: 1.14-fold decrease, $p < .01$, CA1: 1.56-fold decrease, CA2: 6.38-fold decrease, CA3: 4.25-fold decrease; $p < .001$) and continued to decrease in 30 days (DG: 4.69-fold decrease, CA1: 2.39-fold decrease, CA2: 8.28-fold decrease, CA3: 6.19-fold decrease; $p < .001$) and 60 days (DG: 6.36-fold decrease, CA1: 2.93-fold decrease, CA2: 12.72-fold decrease, CA3: 6.78-fold decrease; $p < .001$) exposed group which showed the weakest GR immunoreactivity in different regions of the hippocampus. However, some cells of DG in 15 days exposed group and few cells of CA3 region of all the MW irradiated groups exhibited strong immunoreactivity for GR in addition to majority of cells having reduced immunoreactivity compared with control (Figure 4B). Western blot analysis also confirmed the marked decrease in GR expression in the hippocampus of all the exposed groups (15, 30, and 60 days exposed group, $p < .001$) of mice compared with control (Figure 3B).

We have previously shown that 2.45 GHz MW radiation induces oxidative and nitrosative stress in hippocampus. We chose to investigate i-NOS levels as a marker for hippocampal

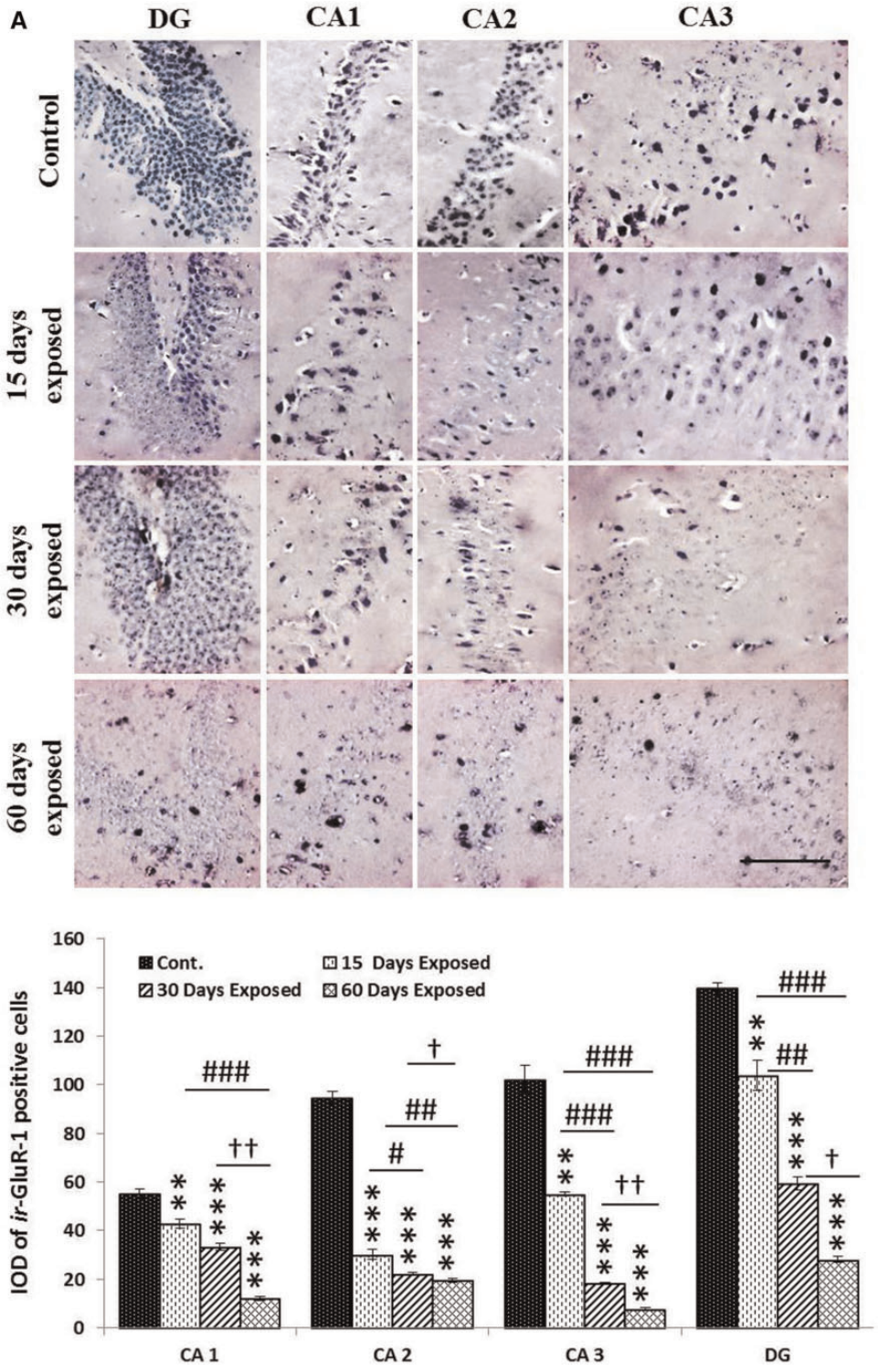

Figure 5. Immunohistochemistry and the IOD of (A) GluR-1 and (B) GluR-2 in CA1, CA2, CA3, and DG regions of hippocampus of mice exposed to 2.45 GHz MW radiation for different duration: Control groups are showing strong/intense immunoreactivity for GluR-1 and GluR-2 in neuronal and nonneuronal cells of all the regions of hippocampus. Note gradual decrease in the number of immunopositive neuronal and nonneuronal cells and their immunoreactivity for GluR-1 and GluR-2 with the increasing duration of MW exposure (control >15 >30 > 60 days). Remarkable reduction in the number of *ir*-neurons and their immunosignaling is evident irreversibly in all the regions of hippocampus in the 60 days exposed group. Scale bar = 50 μm. Values are expressed as mean ± SEM (n = 10). $^{**}p < .01$, $^{***}p < .001$ significance of difference from control; $^{\#}p < .05$, $^{\#\#}p < .01$, $^{\#\#\#}p < .001$ significance of difference from 15 days exposed group; $^{\dagger}p < .05$, $^{\dagger\dagger}p < .01$ significance of difference from 30 days exposed group.

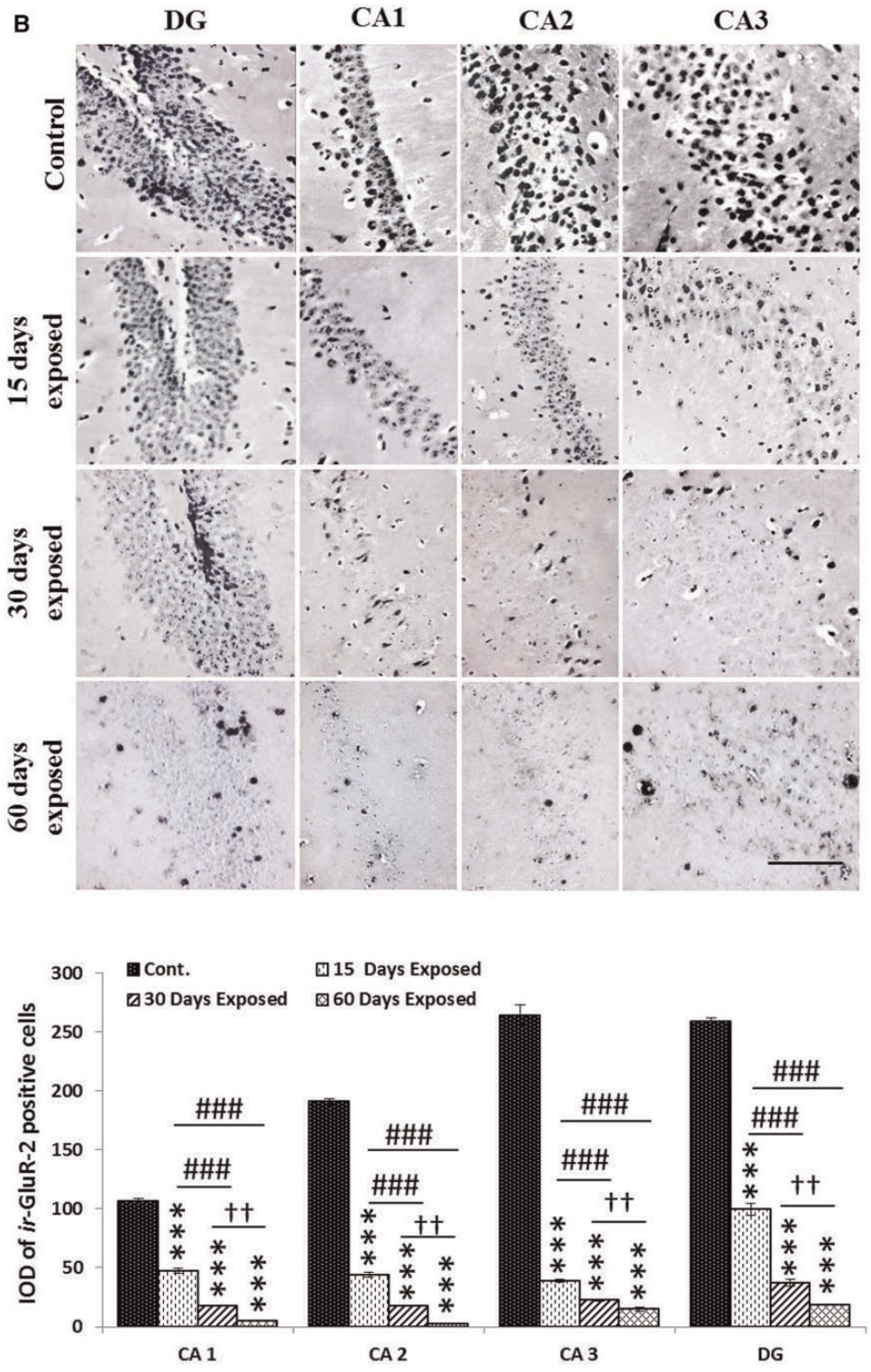

Figure 5. Continued

stress. Using immunofluorescence, we found that i-NOS immunoreactivity was increased in 15 days exposed mice compared with control (DG: 4.2-fold increase, CA1: 1.91-fold increase, $p < .01$, CA2: 1.79-fold increase, CA3: 2.18-fold increase; $p < .001$) (Figure 4C). Similarly, i-NOS reactivity was increased in 30 days (DG: 4.52-fold increase, CA1: 2.79-fold increase, CA2: 2.22-fold increase, CA3: 3.06-fold increase; $p < .001$) and 60 days exposed groups (DG: 7.89-fold increase, CA1: 3.53-fold increase, CA2: 2.89-fold increase, CA3: 7.14-fold increase; $p < .001$) in all hippocampal regions compared with control. Thus, MW irradiation increased the levels of serum corticosterone and CRH, CRH-R1, and i-NOS immunoreactivity in a duration dependent manner,

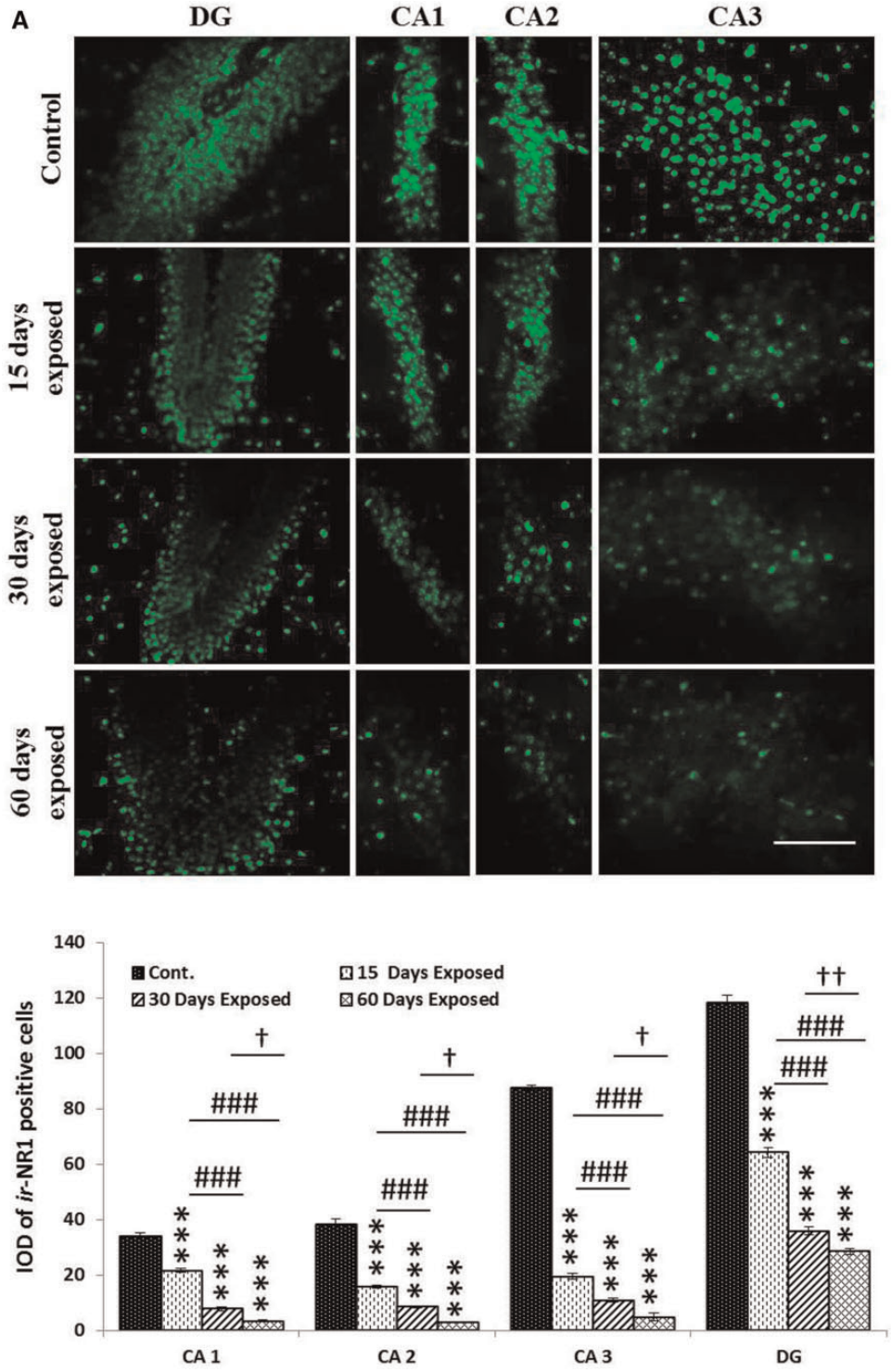

Figure 6. Immunofluorescence and the IOD of N-methyl-D-aspartate (NMDA) receptors (A) NMDA R1 (NR1), (B) NMDA R2A (NR2A) and (C) NMDA R2B (NR2B) in CA1, CA2, CA3, and DG regions of hippocampus of mice exposed to 2.45 GHz MW radiation for different duration: Control group revealed very strong/intense immunoreactivity for NR1, NR2A, and NR2B in large number of neuronal and nonneuronal cells in all the regions of hippocampus. Fifteen days exposed group revealed moderate immunoreactivity in less number of less number of neuronal and nonneuronal cells while 30 and 60 days exposed groups show weak and weaker immunoreactivity, respectively. Moreover, the number of immunopositive cells also decreased in these groups compared with their respective control. Scale bar = 50 μm. Values are expressed as mean ± SEM (n = 10). $^{*}p < .05$, $^{**}p < .01$, $^{***}p < .001$ significance of difference from control; $^{\#}p < .05$, $^{\#\#}p < .01$, $^{\#\#\#}p < .001$ significance of difference from 15 days exposed group; $^{\dagger}p < .05$, $^{\dagger\dagger}p < .01$, $^{\dagger\dagger\dagger}p < .001$ significance of difference from 30 days exposed group.

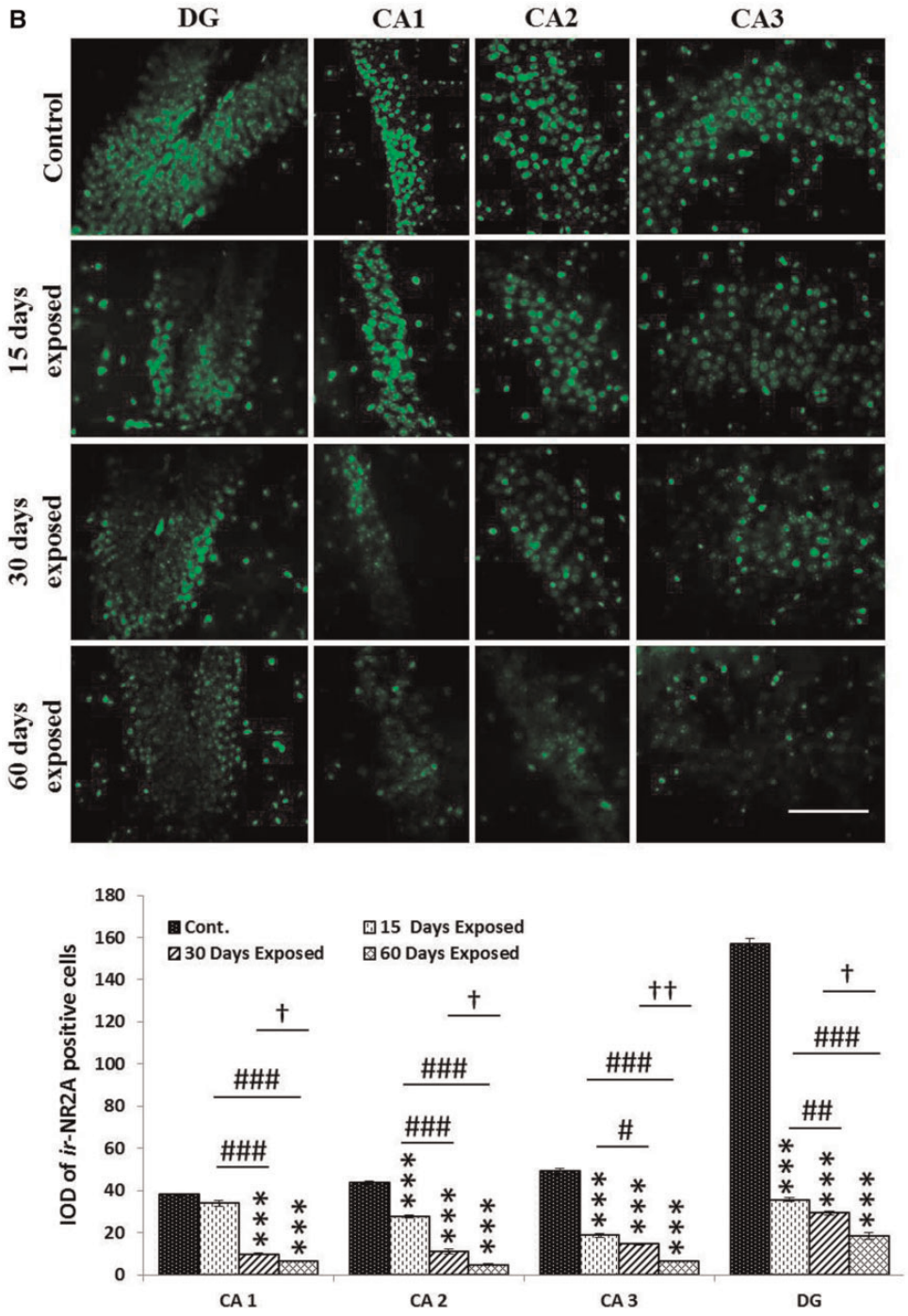

Figure 6. Continued

but resulted in decrease of GR immunoreactivity. Taken together these data show that MW radiation causes hippocampal stress and alters expression of stress-proteins.

CW 2.45 GHz MW Irradiation Decreased the Expression of iGluRs in the Hippocampus of Mice

Having characterized hippocampal stress during MW irradiation, we next asked if MW irradiation causes changes in hippocampal neuronal function and synaptic plasticity. We chose to profile the protein expression levels of 2 iGluRs—NMDA and AMPA receptors as they act as coincidence detectors for synaptic plasticity. Although AMPA receptors are the main charge carriers during basal transmission and permit the influx of Na^+ thereby depolarizing the postsynaptic membrane, NMDA receptors, blocked by magnesium ions, permit only ion flux following prior depolarization. The expression of GluR1, GluR2, NR1, NR2A, and NR2B was found to downregulated in the subregions of hippocampus of all the 2.45 GHz MW irradiated mice. When compared with control which shows strong immunoreactivity for GluR1 (Figure 5A), GluR2 (Figure 5B), NR1 (Figure 6A), NR2A

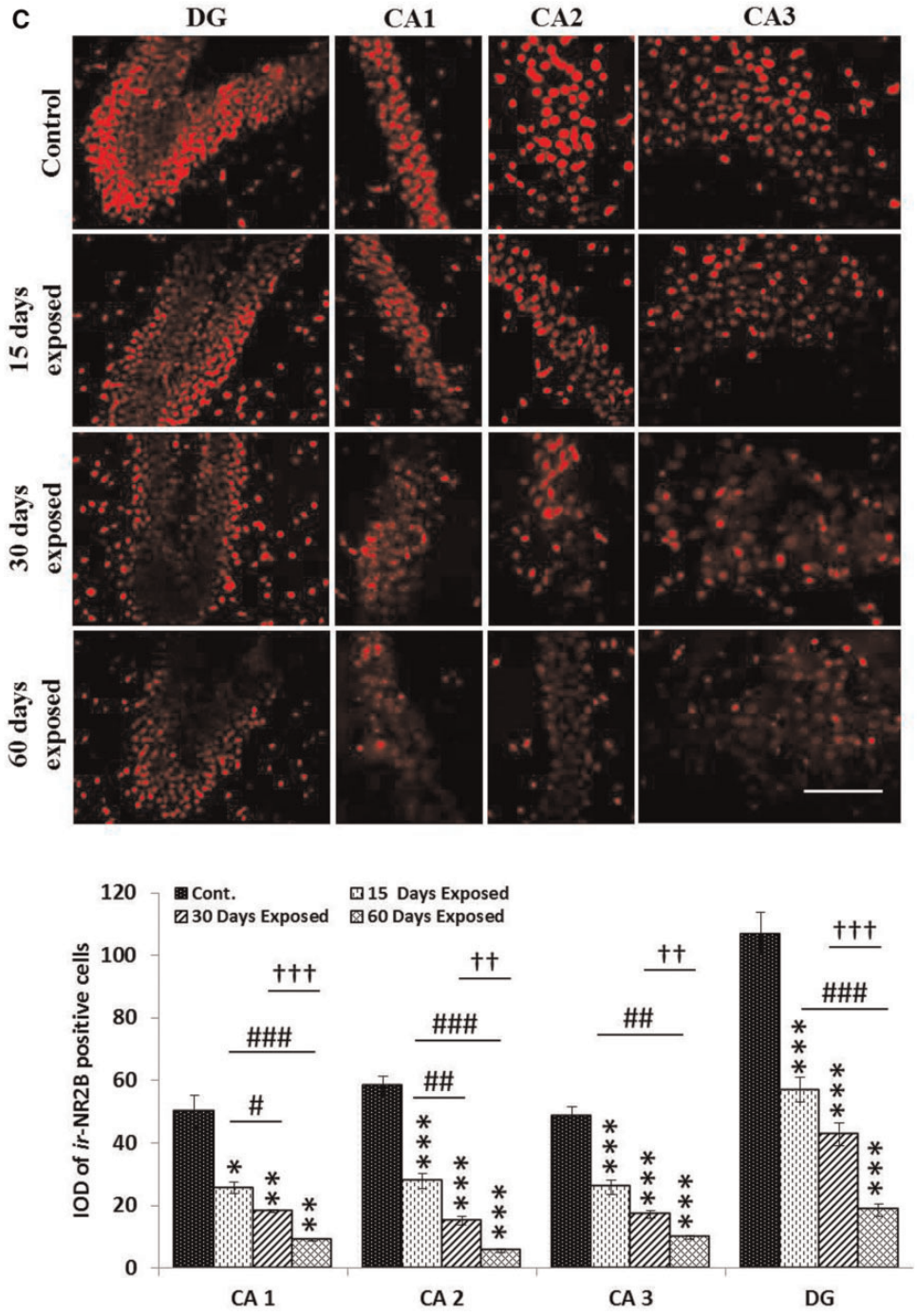

Figure 6. Continued

(Figure 6B), and NR2B (Figure 6C) in large number of neurons, 15 days exposed group shows moderate (GluR1: DG: 1.35-fold decrease, $p < .01$; CA1: 1.29-fold decrease, $p < .01$; CA2: 3.13-fold decrease, $p < .001$; CA3: 1.86-fold decrease, $p < .01$; GluR2: DG: 2.59-fold decrease, CA1: 2.25-fold decrease, CA2: 4.34-fold decrease, CA3: 6.81-fold decrease; $p < .001$; NR1: DG: 1.84-fold decrease, CA1: 1.57-fold decrease, $p < .01$, CA2: 2.43-fold decrease, CA3: 4.49-fold decrease, $p < .001$; NR2A: DG: 4.41-fold decrease, $p < .001$; CA1: 1.12-fold decrease, CA2: 1.58-fold decrease, $p < .001$; CA3: 2.63-fold decrease; $p < .001$; NR2B: DG: 1.88-fold decrease, $p < .001$ CA1: 1.96-fold decrease, $p < .05$; CA2: 2.1-fold decrease, $p < .001$; CA3: 1.88-fold decrease, $p < .001$) while 30 days (GluR1: DG: 2.35-fold decrease, CA1: 1.65-fold decrease, CA2: 3.28-fold decrease, CA3: 5.58-fold decrease, $p < .001$; GluR2: DG: 6.93-fold decrease, CA1: 5.95-fold decrease, CA2: 10.63-fold decrease, CA3: 11.58-fold decrease, $p < .001$; NR1: DG: 3.29-fold decrease, CA1: 4.32-fold decrease, $p < .01$, CA2: 4.42-fold decrease, CA3: 8-fold decrease, $p < .001$; NR2A: DG: 5.37-fold decrease, CA1: 3.88-fold decrease, CA2: 3.97-fold decrease, CA3: 3.34-fold decrease, $p < .001$; NR2B: DG: 2.5-fold decrease, CA1:

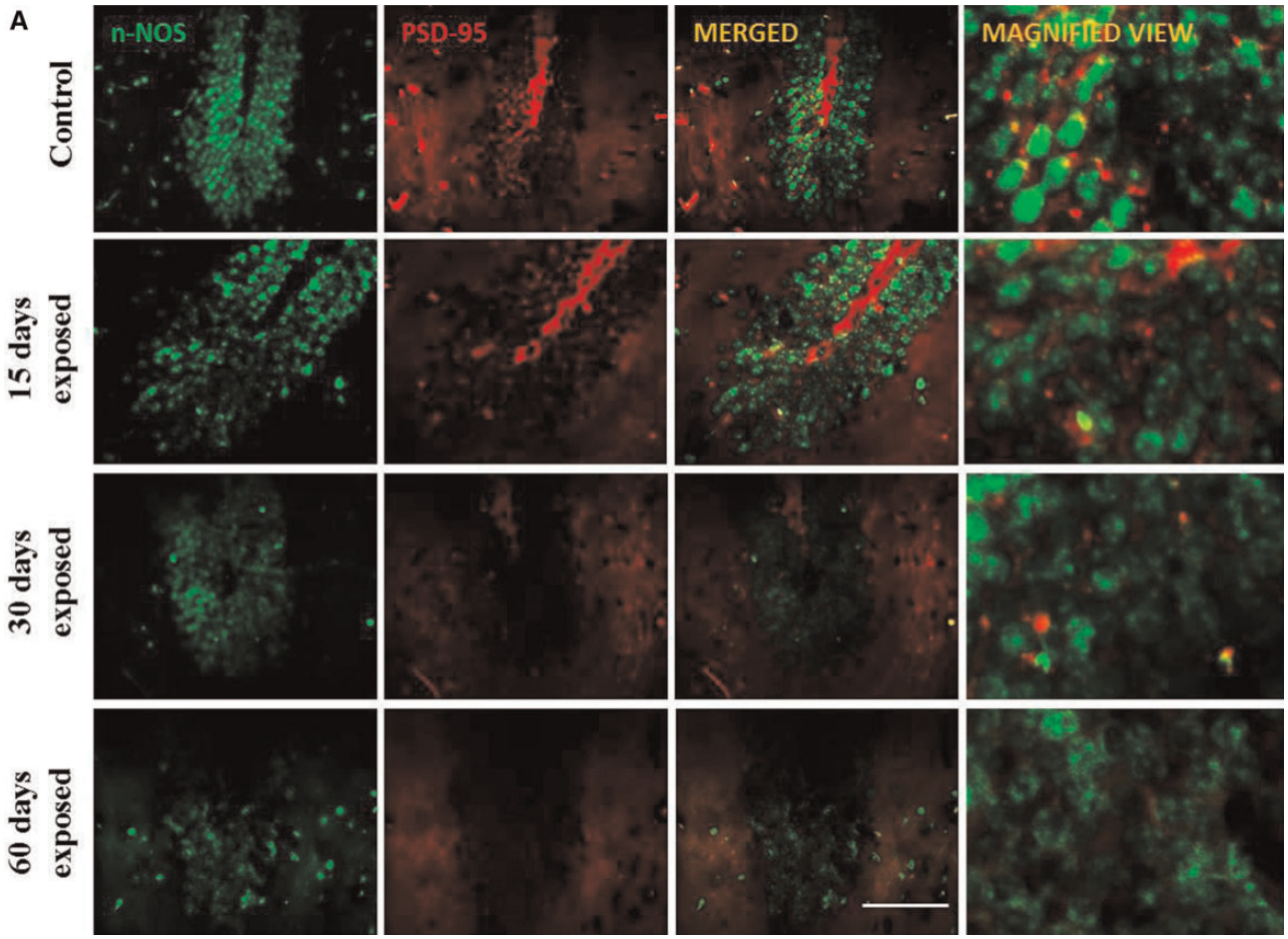

Figure 7. Immunofluorescence showing the co-expression of n-NOS and PSD-95 (A–C) and the IOD of n-NOS and PSD-95 in DG, CA1, and CA3 region of hippocampus of mice exposed to 2.45 GHz MW radiation for different duration: Note intense immunoreactivity for n-NOS as well as PSD-95 in control group while 15 days exposed group shows moderate and 30 as well as 60 days exposed groups show weak immunoreactivity for n-NOS and PSD-95 in all the regions of hippocampus. Scale bar = 50 μm. Values are expressed as mean ± SEM (n = 10). $^{*}p < .05$, $^{**}p < .01$, $^{***}p < .001$ significance of difference from control; $^{\#\#}p < .01$, $^{\#\#\#}p < .001$ significance of difference from 15 days exposed group; $^{\dagger\dagger}p < .01$, $^{\dagger\dagger\dagger}p < .001$ significance of difference from 30 days exposed group.

2.76-fold decrease, CA2: 3.86-fold decrease, CA3: 2.86-fold decrease, $p < .001$) and 60 days (GluR1: DG: 4.98-fold decrease, CA1: 4.57-fold decrease, CA2: 4.86-fold decrease, CA3: 13.11-fold decrease, $p < .001$; GluR2: DG: 13.99-fold decrease, CA1: 21.36-fold decrease, CA2: 66.53-fold decrease, CA3: 17.89-fold decrease, $p < .001$; NR1:- DG: 4.15-fold decrease, CA1: 9.89-fold decrease, CA2: 12.74-fold decrease, CA3: 18.06-fold decrease, $p < .001$; NR2A: DG: 8.51-fold decrease, CA1: 5.98-fold decrease, CA2: 9.17-fold decrease, CA3: 7.45-fold decrease, $p < .001$; NR2B: DG: 5.75-fold decrease, CA1: 5.55-fold decrease, CA2: 10.48-fold decrease, CA3: 4.97-fold decrease, $p < .001$) exposed group shows weak immunoreactivity and in relatively less number of neurons in different regions of hippocampus.

CW 2.45 GHz MW Irradiation Decreased the Expression of Downstream Signaling Molecules Involved in the Memory Formation Pathway in the Hippocampus of Mice

We further checked the alteration in the downstream signaling molecules, involved in the memory formation pathway, due to short and long term 2.45 GHz MW radiation induced stress responses. Using double immunofluorescence, we observed that the control group showed strong immunoreactivity for both n-NOS and PSD-95 which decreased gradually in DG region of hippocampus of 15, 30, and 60 days MW exposed mice (Figure 7A). Similar to hippocampal DG region, CA1 (Figure 7B) and CA3 (Figure 7C) regions of hippocampus showed intense immunoreactivity in n-NOS and PSD-95 positive cells in control group, but remarkable decrease was evident in 15 days exposed group (n-NOS: DG: 1.35-fold decrease, CA1: 1.61-fold decrease, CA3: 4.51-fold decrease, $p < .001$; PSD-95: DG: 1.5-fold decrease, $p < .05$; CA1: 2.33-fold decrease, $p < .05$; CA3: 1.42-fold decrease, $p < .01$) which continued further in 30 days (n-NOS: DG: 2.79-fold decrease, CA1: 4.89-fold decrease, CA3: 8.72-fold decrease, $p < .001$; PSD-95: DG: 2.75-fold decrease, CA1: 16.86-fold decrease, CA3: 2.44-fold decrease, $p < .001$) and 60 days (n-NOS: DG: 5.76-fold decrease, CA1: 13.24-fold decrease, CA3: 22.23-fold decrease, $p < .001$; PSD-95: DG: 15.47-fold decrease, CA1: 77.47-fold decrease, CA3: 4.15-fold decrease, $p < .001$) MW exposed mice hippocampus subdivisions. Co-expression of n-NOS and PSD-95 shows that not only the number of both the types of immunopositive cells but the association between these 2 also decreased with the increased duration of exposure in duration dependent manner (Figs. 7A–C).

Further, compared with strong immunoreactivity for PKCε (Figure 8A), PKA (Figure 8B), ERK1/2 (Figure 8C), and p-ERK1/2 (Figure 8D) in large number of neurons in DG, CA1, CA2, and

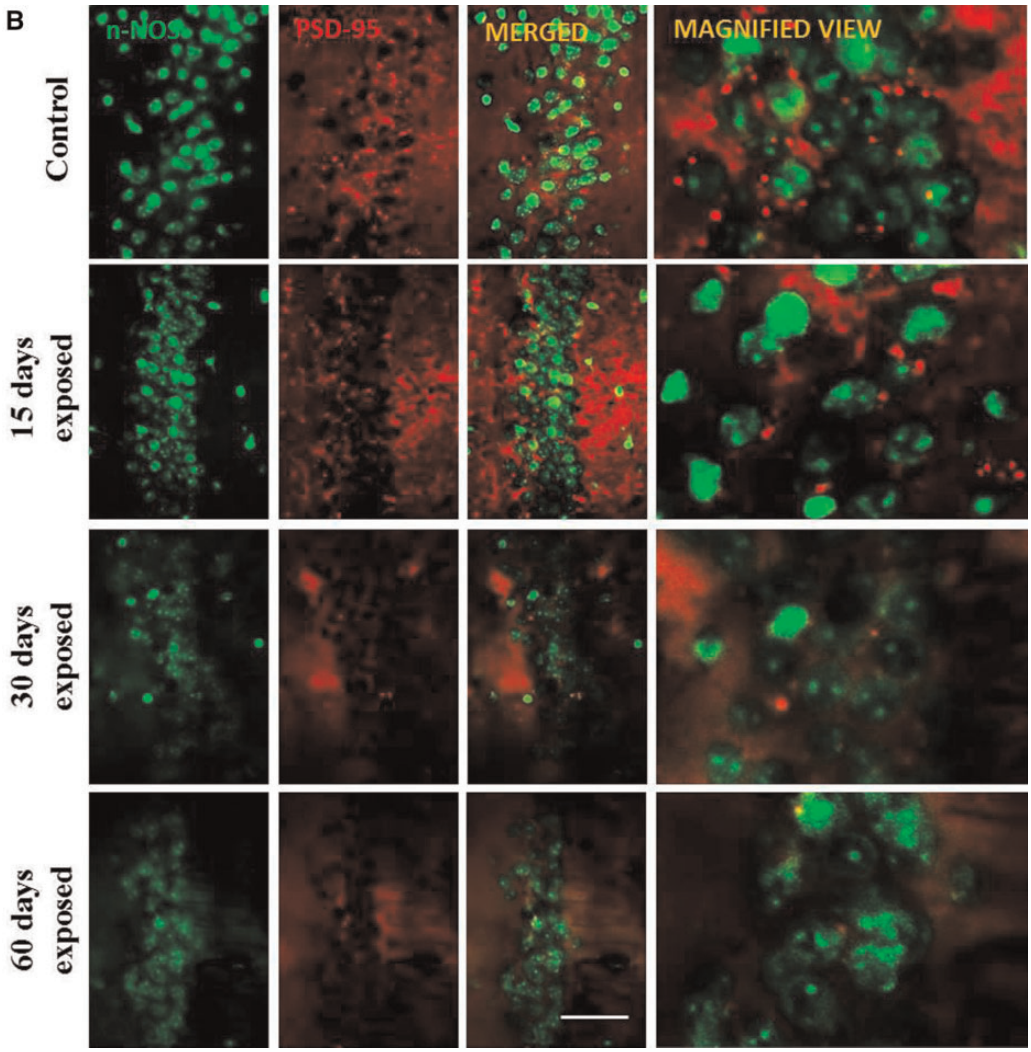

Figure 7. Continued

CA3 regions of hippocampus of the control group, 15 days exposed group shows moderate immunoreactivity in less number of neurons (PKCε: DG: 2.75-fold decrease, CA1: 2.13-fold decrease, CA2: 1.93-fold decrease, CA3: 3.86-fold decrease, $p < .001$; PKA: DG: 1.89-fold decrease, CA1: 1.72-fold decrease, CA2: 3.12-fold decrease, CA3: 1.67-fold decrease, $p < .001$; ERK1/2: DG: 2.56-fold decrease, CA1: 1.52-fold decrease, CA2: 2.6-fold decrease, CA3: 3.14-fold decrease, $p < .001$; p-ERK1/2: DG: 1.54-fold decrease, CA1: 2.27-fold decrease, CA2: 1.79-fold decrease, CA3: 6.2-fold decrease; $p < .001$), while 30 days (PKCε: DG: 4.1-fold decrease, CA1: 3.17-fold decrease, CA2: 2.74-fold decrease, CA3: 3.84-fold decrease, $p < .001$; PKA: DG: 4.27-fold decrease, CA1: 3.15-fold decrease, CA2: 3.58-fold decrease, CA3: 3.44-fold decrease; $p < .001$; ERK1/2: DG: 5.27-fold decrease, CA1: 2.93-fold decrease, CA2: 3.15 fold decrease, CA3: 3.42 fold decrease, $p < .001$; p-ERK1/2: DG: 3.04-fold decrease, CA1: 6.15-fold decrease, CA2: 7.99-fold decrease, CA3: 8.19-fold decrease; $p < .001$) and 60 days (PKCε: DG: 7.26-fold decrease, CA1: 5.22-fold decrease, CA2: 4.41-fold decrease, CA3: 5.36-fold decrease, $p < .001$; PKA: DG: 6.25-fold decrease, CA1: 5.64-fold decrease, CA2: 11.38-fold decrease, CA3: 4.56-fold decrease; $p < .001$; ERK1/2: DG: 2.9-fold decrease, CA1: 6.43-fold decrease, CA2: 4.96-fold decrease, CA3: 6.44-fold decrease, $p < .001$; p-ERK1/2: DG: 6.71-fold decrease, CA1: 7.98-fold decrease, CA2: 10.28-fold decrease, CA3: 11.94-fold decrease; $p < .001$) exposed group revealed weak immunoreactivity in some neurons only. The expression of CREB and p-CREB was found to be decreased significantly in the hippocampus of 15 (CREB: $p < .05$; p-CREB: $p < .001$) 30 (CREB: $p < .01$; p-CREB: $p < .001$) and 60 days (CREB: $p < .001$; p-CREB: $p < .001$) exposed group of mice compared with respective controls (Figure 3B).

DISCUSSION

Our previous report clearly demonstrates that CW 2.45 GHz MW radiation induced oxidative and nitrosative stress induces damage to cellular constituents (viz., nucleic acids, proteins, and lipids) and results in the hippocampal neuronal and nonneuronal apoptosis. Moreover, we also found that the apoptosis followed p53 dependent/independent, Bax mediated and caspase-induced pathway. Hence, in our previous study, we have concluded that CW 2.45 GHz MW radiation triggers the hippocampal neuronal and nonneuronal cell death via inducing oxidative/nitrosative stress and leads to subsequent loss in

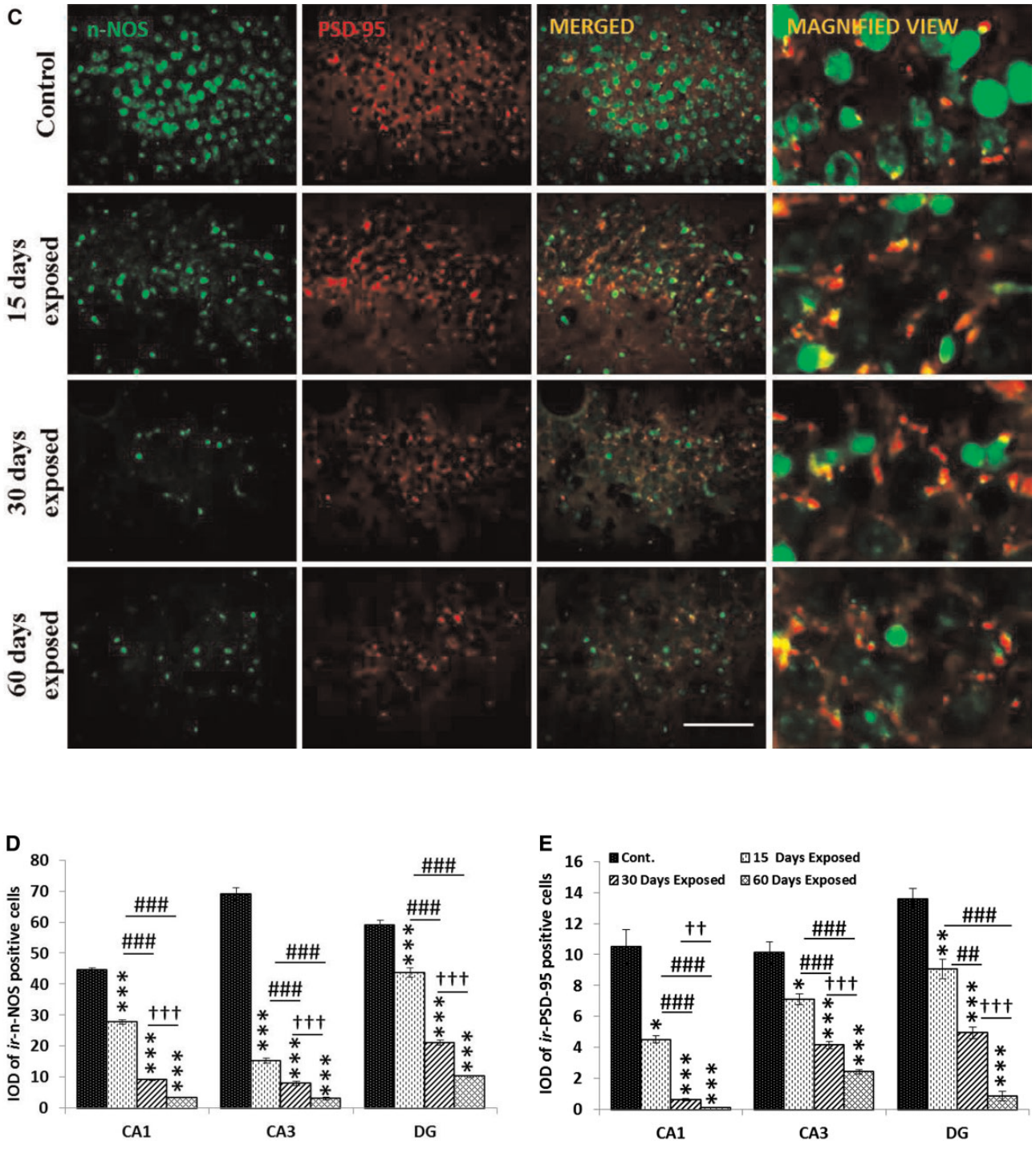

Figure 7. Continued

learning and spatial memory. To assess the effect of CW 2.45 GHz MW radiation on hippocampal learning and memory consolidation and to strengthen our previous MWM data, we have performed the 8-RAM test in 2.45 GHz MW exposed mice for different time duration, ie, 15, 30, and 60 days. Mice exposed to 2.45 GHz MW radiation revealed pronounced spatial memory impairment in RAM task. Thirty and sixty days exposed mice were very slow to learn the baited and unbaited arms and showed significantly increased number of reference and WMEs during the training period. They also revealed reduced memory consolidation as evident by decreased performance rate (a combination of working and RMEs to measure the neural involvement in memory formation and spatial learning retrieval on RAM [Nikbakht *et al.*, 2012]) and percent time spent in previously baited arms.

Further in this direction, and to understand the underlying molecular mechanism(s) of memory deficit, we have investigated the effect of 2.45 GHz MW radiation on GluRs and various

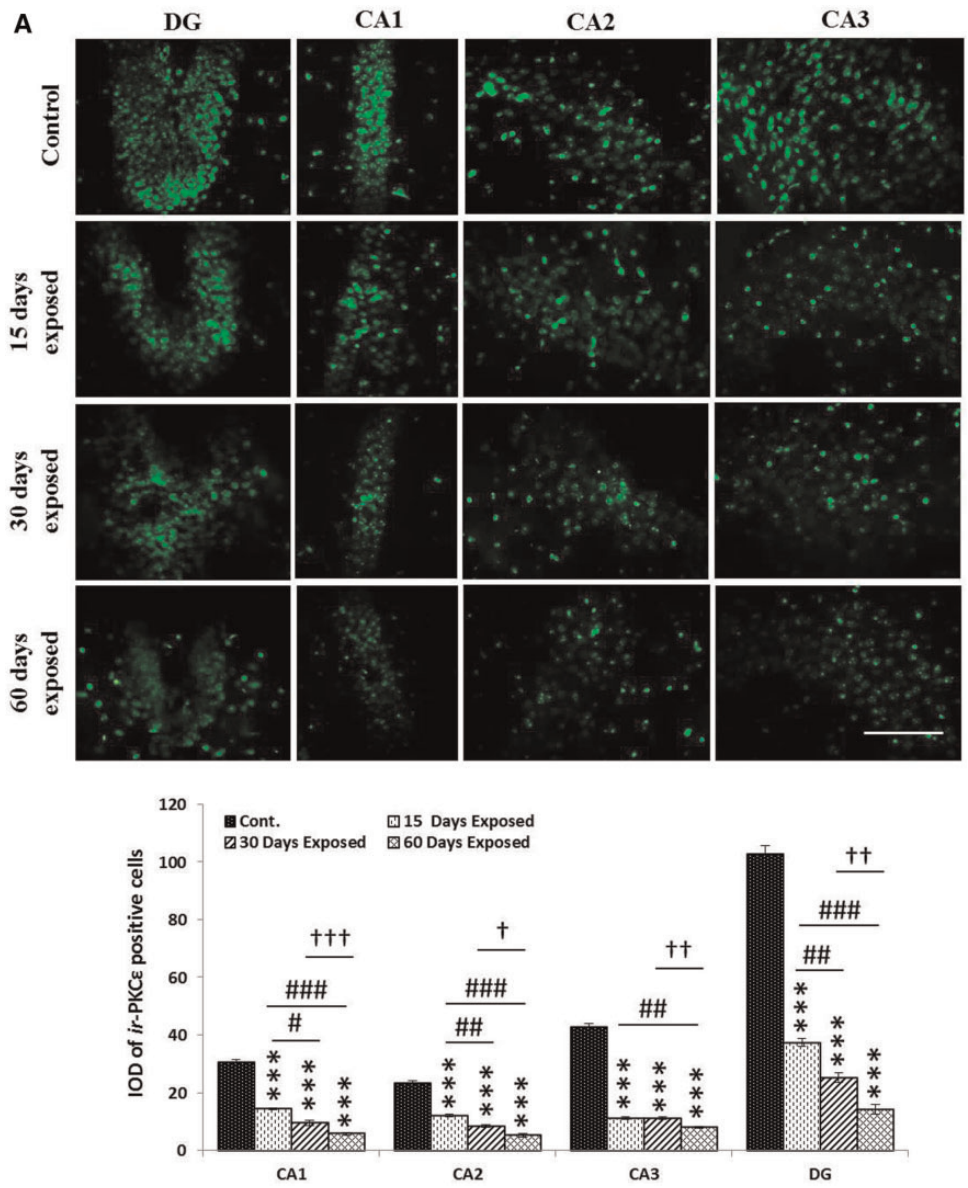

Figure 8. Immunofluorescence and the IOD of (A) PKCε, (B) PKA, (C) ERK ½, and (D) p-ERK in CA1, CA2, CA3 and DG regions of hippocampus of mice exposed to 2.45 GHz MW radiation for different duration: Control group shows strong/intense immunoreactivity for PKCε, PKA, ERK1/2, and p-ERK in large number of neuronal and non-neuronal cells. 15 and 30 days exposed group shows moderate and weak immunoreactivity for PKCε, PKA, ERK1/2, and p-ERK, respectively in less number of cells. However, in 60 days exposed group only few numbers of cells are immunopositive and showing weak immunoreactivity for PKCε, PKA, ERK1/2, and p-ERK compared with their respective controls. Scale bar = 50 μm. Values are expressed as mean ± SEM (n = 10). $^{***}p < .001$ significance of difference from control; $^{\#}p < .05$, $^{\#\#}p < .01$, $^{\#\#\#}p < .001$ significance of difference from 15 days exposed group; $^{\dagger}p < .05$, $^{\dagger\dagger}p < .01$, $^{\dagger\dagger\dagger}p < .001$ significance of difference from 30 days exposed group.

other signaling molecules involved in memory formation pathway. Our results demonstrate that 2.45 GHz MW radiation exposure for different time durations (15, 30, and 60 days) significantly increased the expression of CRH and CRH-R1 along with significantly decreased expression of GR in all the hippocampal subregions ie, DG, CA1, CA2 and CA3 of mice. This might have occurred due to MW radiation induced oxidative and nitrosative stress resulting into the activation of HPA axis and hippocampal local stress circuitry (increased hippocampal CRH and decreased GR). Increased serum corticosterone level, the outcome of activated HPA axis may lead to the reduced hypothalamic GR expression. But the 2 h/d chronic stress in case of 2.45 GHz MW radiation results in duration dependent rise in serum corticosterone. Further, some common chronic stressors such as repetitive social stressors, or chronic corticosterone injections, chronic immobilization as well as unpredictable randomized stressors have been reported to mediate hippocampal-dependent memory deficits (Liu *et al.*, 2012). Hence, 2.45 GHz MW radiation like other chronic stressors seems to affect the hippocampal dependent learning and spatial memory formation processes.

Severe acute or chronic stress exposure like 2.45 GHz MW radiation can also be deleterious to the hippocampal neuronal morphology. The apoptotic loss of hippocampal neurons, dendritic atrophy, decreased spine number and branch length (Shahin *et al.*, 2015) may be due to the action of corticosterone via GRs and/or increased CRH-CRH-R1 expression in all the hippocampal subregions (CA1, CA2, CA3, and DG) of 2.45 GHz MW

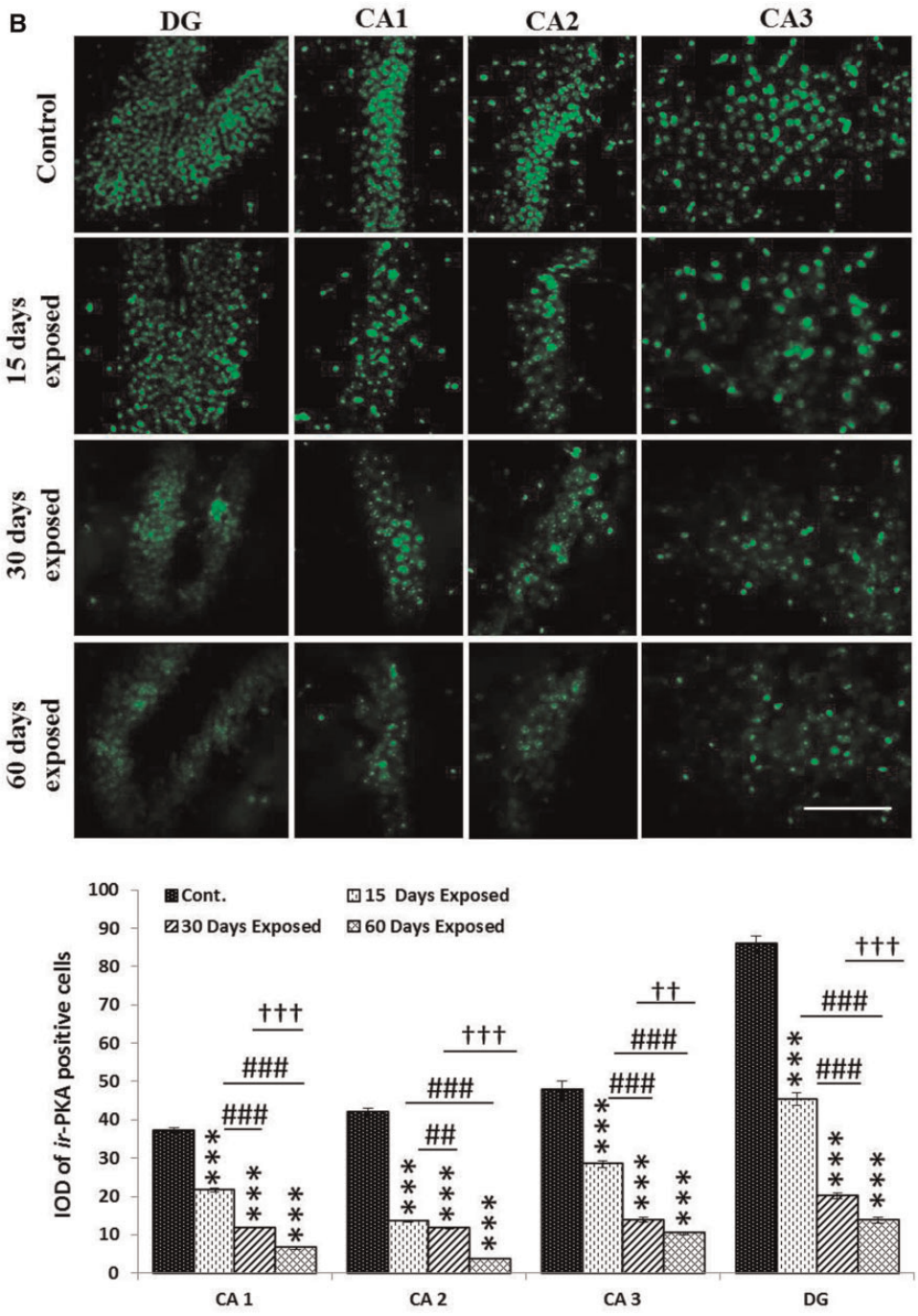

Figure 8. Continued

radiation exposed groups of mice. Chronic stress or corticosterone administration is also reported to induce atrophy of dendrites in the CA1, CA3, and DG (McEwen, 2000; Vyas *et al.*, 2002), as well as loss of excitatory synapses in the CA3 area (Sousa *et al.*, 2000). It is also well documented that GC treatment causes extensive dendritic atrophy and stress-induced atrophy is prevented by using adrenal steroidogenesis blockers (Magariños and McEwen, 1995). Hence, stress induced increase in endogenous GCs may play a role in stress-induced dendritic atrophy. Thus, the severe or chronic stress contributes in dramatic changes in hippocampal neuronal cytoarchitechture and physiology and in turn may alter the specific memory-based behavioral responses in 2.45 GHz MW radiation exposed groups.

Previous studies in hippocampal organotypic cultures, treated with CRH chronically (1–2 weeks), shows impoverished dendritic arborization and reduced total dendritic length implicating the role of CRH signaling in stress-induced morphological changes (Chen *et al.*, 2013; Joëls, 2008). Our studies suggest that MW radiation induced stress could result in structural and functional changes of hippocampal neurons that are either

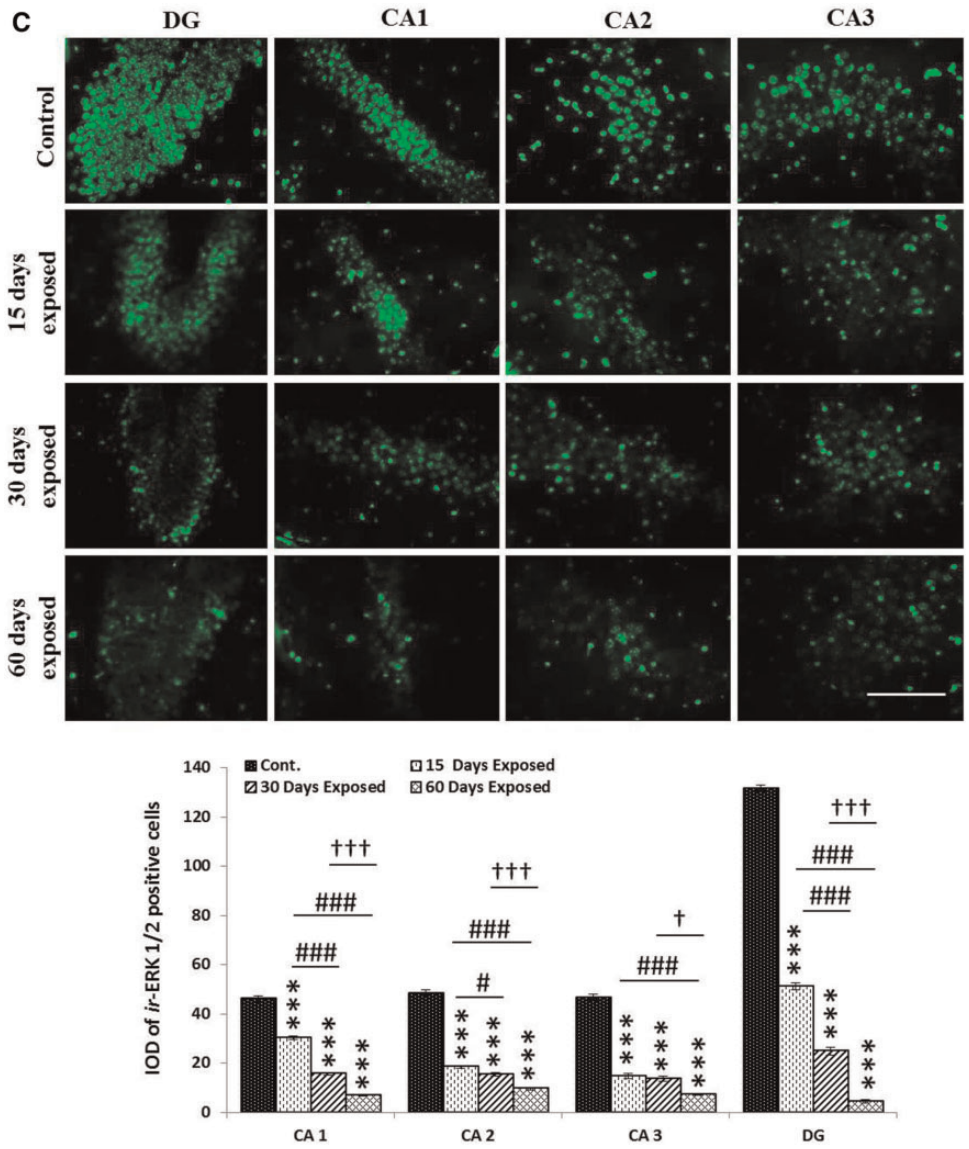

Figure 8. Continued

mediated independently by CRH and GCs or via their interactions with the signaling pathways within the hippocampus. However, our results suggest possible interactions with the signaling pathways as seen by the cumulative increase in the expression of CRH-CRHR1 in hippocampal subregions and increased serum corticosterone levels. The 2.45 GHz MW radiation induced loss of post synaptic iGluRs (NMDA and AMPA receptor subunits) seems to be mediated through the coupled action of CRH-CRHR1 and corticosterone-GR.

Glutamate induced activation of AMPA receptor subunits, especially GluR1/R2-mediated generation of the postsynaptic membrane depolarization activate the NMDA receptor subunits and stimulate the intracellular Ca^{2+} level and subsequently develop postsynaptic potential and thus potentiate synaptic plasticity, LTP formation and stabilization. Our study shows that temporal exposure to 2.45 GHz MW radiation leads to significantly decreased expression of NMDA receptor subunits (NR1, NR2A, and NR2B) and AMPA receptor subunits (GluR1 and GluR2) in all the hippocampal regions—CA1, CA2, CA3, and DG. Decreased expression of NMDA and AMPA receptor subunits upon MW radiation in turn reduce the excitatory inputs in the neurons required in the LTP formation. These observations are consistent with the findings of Wang and group (Wang *et al.*, 2015). They shows that MW radiation exposure decreased the amino acid neurotransmitters level, glutamate and gammaaminobutyric acid (GABA) ratio as well as NMDA receptor subunits (NR1 and NR2B) expression in the hippocampus of rat brain. Other report also suggest that long-term exposure to MW may impaired spatial learning and memory in dose-dependent manner via inhibiting brain electrical activity, inducing hippocampus neuronal degeneration and altering neurotransmitters level (Li *et al.*, 2015). Although, some study suggest the MW radiation induced over-activation of NMDAR and increased glutamic acid and GABA ratio was associated with synaptic plasticity impairment (Xiong *et al.*, 2015).

We also found reduced expression of PSD-95 in all the hippocampal subregions of MW irradiated, consistent with other

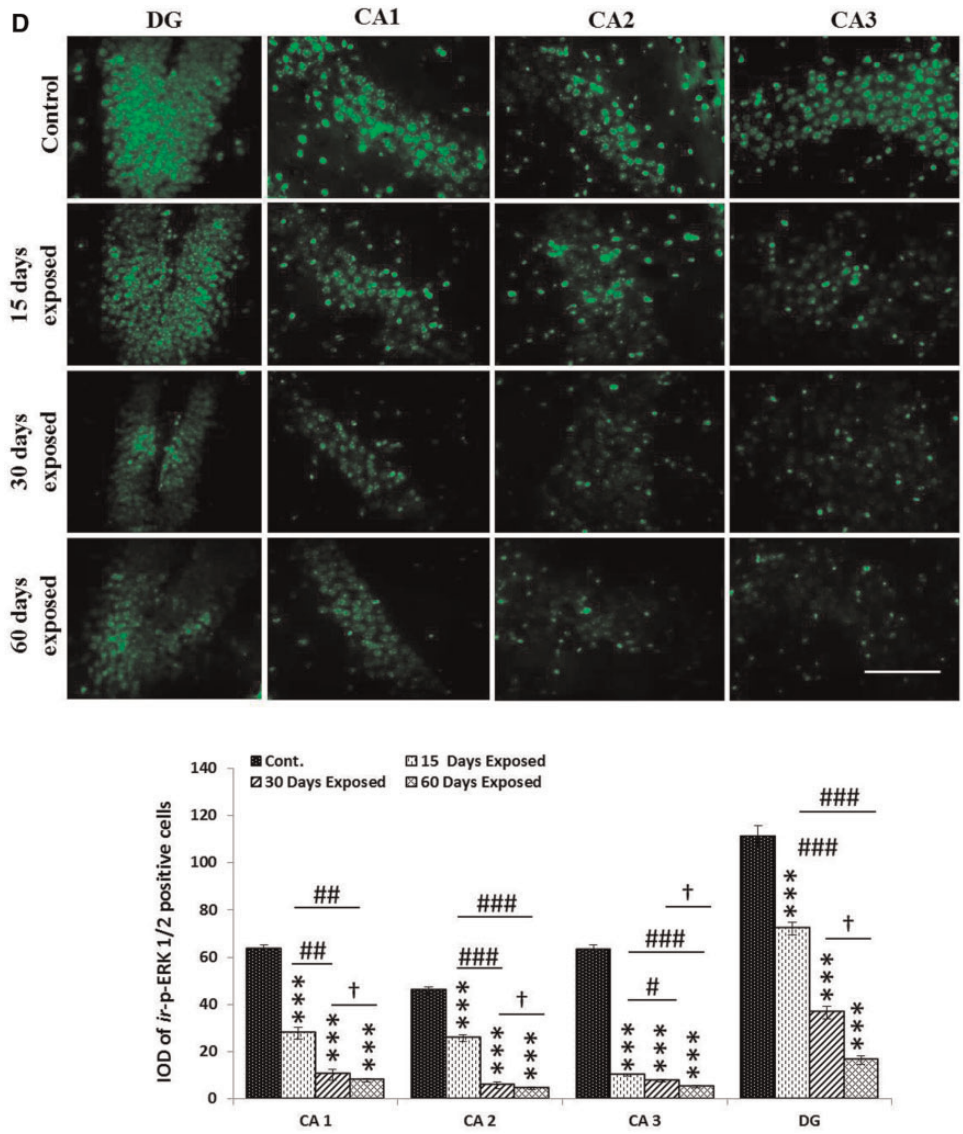

Figure 8. Continued

studies reporting the stress induced loss of PDZ family proteins in hippocampus (Cohen *et al.*, 2011). Our results also showed decreased expression of PKCε, PKA ERK/p-ERK, and CREB/p-CREB in all the hippocampal subregions of MW irradiated mice suggesting that MW radiation suppresses the PKCε/PKA mediated neuronal processes and pathways related to LTP formation and stabilization. The role of PKCε and PKCα in learning and memory has been extensively studied (Hongpaisan *et al.*, 2007; Sun *et al.*, 2008). PKCε and PKCα is also associated with synaptogenesis, synaptic remodelling and BDNF/NGF mediated neurite outgrowth (Kolkova *et al.*, 2005; Shirai *et al.*, 2008), resulting in a restoration of hippocampus-dependent cognitive functions (Sun *et al.*, 2008). Further the ERK1/2 signaling is essential for transcriptional activation during LTM but not short-term memory formation and also plays essential role in learning and memory (Adams and Sweatt, 2002). The decreased expression of PKCε, PKA, ERK/p-ERK, and CREB/p-CREB upon MW irradiation provides the molecular basis for learning and memory impairment on MW irradiated mice reported previously by our group (Shahin *et al.*, 2015). Although, Zuo and group suggested that 2.856 GHz MW radiation exposure for 5 min induce apoptosis in neuronal cell culture via over activation of MEK/ERK/CREB signaling pathway (Zuo *et al.*, 2015). This study is controversial with our findings may be because of our *in vivo* mouse model, the difference in chronic exposure pattern, the daily duration of 2 h for 15, 30, and 60 days and also in power density used in our study plan.

We also report increased hippocampal NO levels and i-NOS expression in all the hippocampal subregions along with significantly decreased n-NOS levels in 2.45 GHz MW radiation exposed mice. Increased NO levels coupled with hippocampal neural cell death may induce the activation of microglial i-NOS system which also create imbalance between free radicals production and the antioxidant defences (Tran *et al.*, 1997). The increased free radical load (ROS/NO levels) induces LPO and protein carbonylations of hippocampal neuronal/nonneuronal

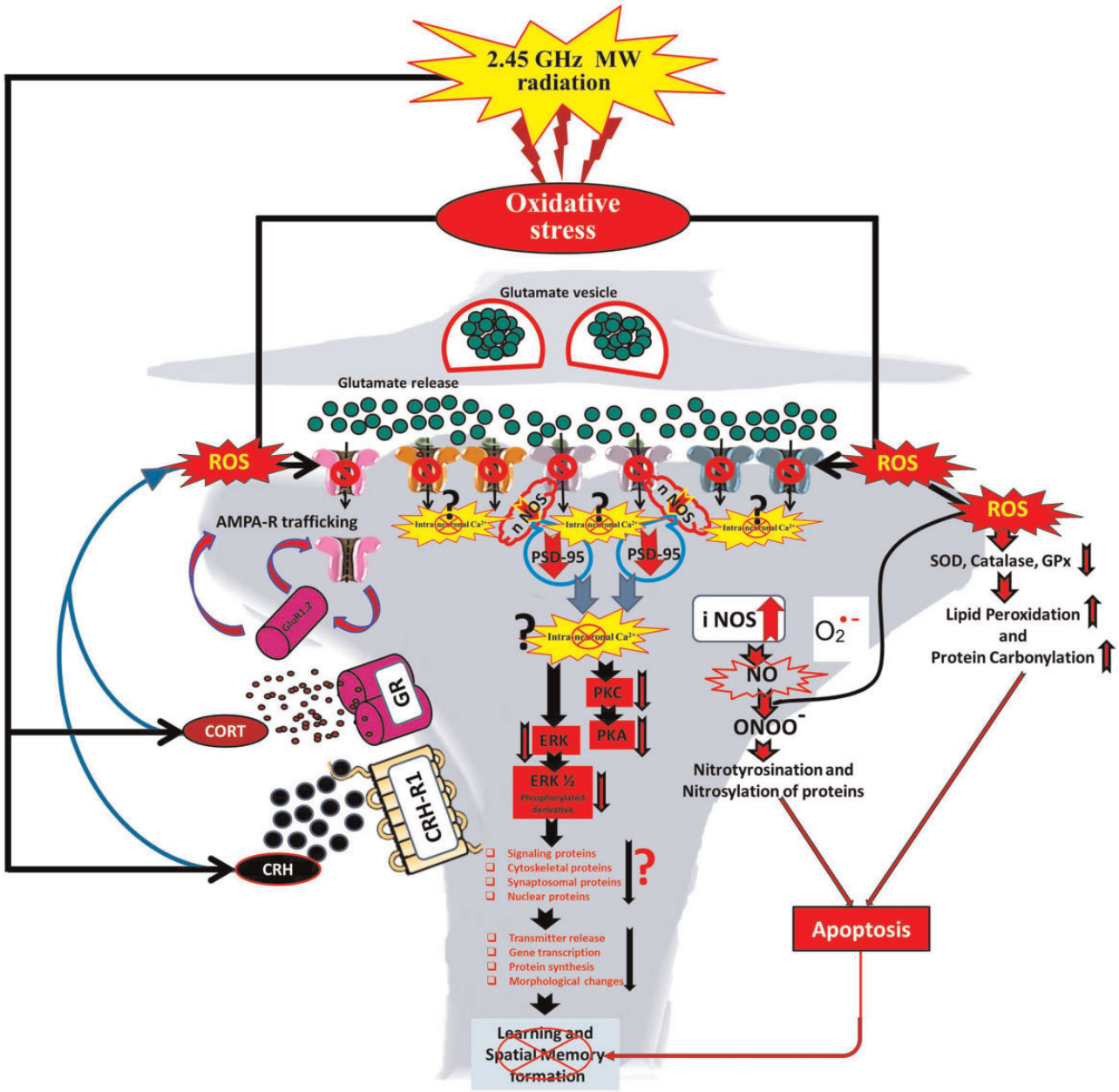

Figure 9. Schematic diagram depicting the 2.45 GHz (CW) MW radiation induced hippocampal stress (hippocampal iNOS-CRH-CRHR1-GR) resulting into hippocampal-based learning and spatial memory impairment via suppressing the iGluR (AMPAR and NMDAR)-nNOS-PSD-95-PKCε-PKA-ERK-pERK-mediated hippocampal memory formation pathway. This model summarizes the findings on disrupted hippocampal-based memory formation pathways leading to impairment of hippocampal-based learning and memory as observed in this study.

cells which may again induce overexpression of i-NOS in activated microglia (Sugama *et al.*, 2013). Neuronal NOS (n-NOS) accounts for NO production in hippocampus, modulates learning and memory under physiological conditions and affects membrane excitability, synapse connection, and neuronal survival under pathological conditions. It also participates in several types of synaptic plasticity, including long-term depression in the cerebellum and striatum and LTP in the hippocampus and cerebral cortex (Centonze *et al.*, 1999; Garthwaite and Boulton, 1995). The optimal level of NO is required for the proper hippocampal functioning. The activation of n-NOS and other Ca^{2+}-dependent enzymes accounts for many of the deleterious effects associated with excessive NMDA receptor activation (Almeida *et al.*, 1998). Since i-NOS involves a gradual increase in the NO production over prolonged period, resulting in long lasting release of NO in large amounts, this may have direct implications for neuronal degeneration and atrophy. Interestingly, NMDAR activates n-NOS postsynaptically; n-NOS subsequently stimulate NO release to presynaptically upregulate the function of the NMDAR. PSD-95 mediates interaction of NMDA receptors with n-NOS (Brenman *et al.*, 1996; Christopherson *et al.*, 1999; Tochio *et al.*, 2000). Hence, our findings are consistent with the literature demonstrating that neurodegeneration is resulted because of close association between

neuroinflammation accompanied by a state of nitrosative stress.

In our previous study, we have demonstrated that 2.45 GHz MW radiation-induced oxidative and nitrosative stress in hippocampus impairs the learning and spatial memory by causing apoptosis of neuronal and nonneuronal cells of hippocampus (Shahin *et al.*, 2015). MW radiation induced stress causes a duration dependent decrease in dendritic arborization, branching and spine density of hippocampal pyramidal neurons which results in hippocampal-based learning and spatial memory deficits. Findings from our study suggest that 2.45 GHz MW radiation induced local hippocampal stress system (hippocampal i-NOS-CRH-CRHR1-GR) is responsible for the impairment of hippocampal learning and spatial memory formation processes through inhibiting the memory formation signaling cascades, in addition to the hippocampal neuronal and nonneuronal apoptosis. The concomitant occurrence of apoptosis and signaling impairment is hence may be speculated as the cumulative underlying mechanism of 2.45 GHz MW radiation induced hippocampal based learning and spatial memory deficits. Looking into the deeper insights of mechanism(s) behind the hippocampal-based learning and spatial memory impairment following 2.45 GHz MW radiation, what we found is MW radiation induced oxidative and nitrosative stress may trigger the local hippocampal stress responses through the corticosterone-hippocampal GR and hippocampal CRH-CRH-R1 pathways. The 2.45 GHz MW radiation induced free radical load may also suppress iGluRs (AMPA and NMDA receptor subtypes) at the glutamatergic synapse and hence, may inhibit the downstream PSD-95-n NOS signaling, downstream memory forming kinases (PKA-PKCε-ERK1/2 and pERK1/2) and the activation of nuclear transcriptional factors (CREB/p-CREB), that are essential for the LTP/LTM formation and stabilization. However, further research is required in this direction to strengthen our findings and to extrapolate these findings in humans.

CONCLUSION

Altogether, this study, for the first time to best of our knowledge, demonstrates the underlying mechanism of 2.45 GHz MW radiation induced impairment of hippocampal-dependent learning and spatial memory formation. This memory deficit appears to be a concomitant result of the hippocampal neuronal and nonneuronal apoptosis (Shahin *et al.*, 2015) as well as suppression of the classical hippocampal memory formation pathway, ie, iGluR-PSD-95-n NOS cascade and PKA-PKCε-ERK-pERK-CREB signaling. Experimental evidences from our study, also confirms the corticosterone mediated activation of local hippocampal stress circuitry (hippocampal iNOS-CRH-CRHR1-GR) is also involved in suppressing the memory signaling cascades. The increased free radical induced oxidative damage and activation of local hippocampal stress circuitry (hippocampal iNOS-CRH-CRHR1-GR) appears to be interrelated and combinatorially induce the hippocampal neuronal/nonneuronal cell death as well as learning and spatial memory deficits through suppressing the memory signaling cascades.

Moreover, in view of the prevalence and pervasiveness of the usage of MW radiation emitting devices in modern life it was high time to explore the mechanism(s) by which this MW radiation impairs the hippocampal-based learning and memory and also to determine the degree of susceptibility of hippocampal memory and memory based behavioral attributes (MWM and RAM test performance) to MW radiation induced stress. Our findings conclusively indicate deleterious effects of CW 2.45 GHz MW radiation on hippocampal-based memory formation pathway/signaling mechanism(s) (Figure 9). All these experimental evidences, cumulatively also led us to conclude that the degree of severity of MW radiation exposure induced adverse effects on hippocampal-based learning and spatial memory formation increases in a duration dependent manner.

SUPPLEMENTARY DATA

Supplementary data are available at *Toxicological Sciences* online.

ACKNOWLEDGMENTS

We are also extremely thankful to Dr Anne-Marie van Dam, Dr Jack E. Bodwell, and Prof. Richard L. Huganir for generous gift of CRH, GR, and GluRs antibodies, respectively.

FUNDING

This work was funded by a research grant (5/10/FR/13/2010-RHN) from the Indian Council of Medical Research (ICMR), New Delhi, India to CMC, ICMR Senior Research Fellowship (45/2/2012-PHY/BMS) to Ms Saba Shahin and CSIR Senior Research Fellowship (09/013(0339)/2010-EMR-I) to Mr Somanshu Banerjee.

REFERENCES

Adams, J. P., and Sweatt, J. D. (2002). Molecular psychology: Roles for the ERK MAP kinase cascade in memory. *Annu. Rev. Pharmacol. Toxicol.* **42**, 135–163.

Albayram, O., Bilkei-Gorzo, A., and Zimmer, A. (2012). Loss of CB1 receptors leads to differential age-related changes in reward-driven learning and memory. *Front. Aging. Neurosci.* **4**, 34.

Almeida, A., Heales, S. J. R., Bolanos, J. P., and Medina, J. M. (1998). Glutamate neurotoxicity is associated with nitric oxide-mediated mitochondrial dysfunction and glutathione depletion. *Brain Res.* **790**, 209–216.

Banerjee, S., Tsutsui, K., and Chaturvedi, C. M. (2016). Apoptosis mediated testicular alteration in Japanese quail (*Coturnix coturnix japonica*) in response to temporal phase relation of serotonergic and dopaminergic oscillations. *J. Exp. Biol.* **219**, 1476–1487.

Bradford, M. M. (1976). Rapid and sensitive method for the quantitation of microgram quantities of protein utilizing the principle of protein-dye binding. *Anal. Biochem.* **72**, 248–254.

Brenman, J. E., Chao, D. S., Gee, S. H., McGee, A. W., Craven, S. E., Santillano, D. R., Wu, Z., Huang, F., Xia, H., Peters, M. F., *et al.* (1996). Interaction of nitric oxide synthase with the postsynaptic density protein PSD-95 and alpha1-syntrophin mediated by PDZ domains. *Cell* **84**, 757–767.

Bressler, J. P., Olivi, L., Cheong, J. H., Kim, Y., Maerten, A., and Bannon, D. (2007). Metal transporters in intestine and brain: Their involvement in metal-associated neurotoxicities. *Hum. Exp. Toxicol.* **26**, 221–229.

Butterfield, D. A., Castegna, A., Lauderback, C. M., and Drake, J. (2002). Evidence that amyloid b-peptide induced lipid peroxidation and its sequelae in Alzheime's disease brain contribute to neuronal death. *Neurobiol. Aging* **23**, 655–664.

Cammarota, M., Bevilaqua, L. R., Barros, D. M., Vianna, M. R., Izquierdo, L. A., Medina, J. H., and Izquierdo, I. (2005).

Retrieval and the extinction of memory. *Cell Mol. Neurobiol.* **25**, 465–474.

Cassel, J. C., Cosquer, B., Galani, R., and Kuster, N. (2004). Whole-body exposure to 2.45 GHz electromagnetic fields does not alter radial-maze performance in rats. *Behav. Brain Res.* **155**, 37–43.

Centonze, D., Gubellini, P., Bernardi, G., and Calabresi, P. (1999). Permissive role of interneurons in corticostriatal synaptic plasticity. *Brain Res. Brain Res. Rev.* **31**, 1–5.

Chen, Y., Kramár, E. A., Chen, L. Y., Babayan, A. H., Andres, A. L., Gall, C. M., Lynch, G., and Baram, T. Z. (2013). Impairment of synaptic plasticity by the stress mediator CRH involves selective destruction of thin dendritic spines via RhoA signaling. *Mol. Psychiatry* **18**, 485–496.

Choe, E. S., and Wang, J. Q. (2001). Group I metabotropic glutamate receptors control phosphorylation of CREB, Elk-1 and ERK via a CaMKII-dependent pathway in rat striatum. *Neurosci. Lett.* **313**, 129–132.

Christopherson, K. S., Hillier, B. J., Lim, W. A., and Bredt, D. S. (1999). PSD-95 assembles a ternary complex with the N-methyl-D-aspartic acid receptor and a bivalent neuronal NO synthase PDZ domain. *J. Biol. Chem.* **274**, 27467–27473.

Cohen, J. W., Louneva, N., Han, L. Y., Hodes, G. E., Wilson, R. S., Bennett, D. A., Lucki, I., and Arnold, S. E. (2011). Chronic corticosterone exposure alters postsynaptic protein levels of PSD-95, NR1, and synaptopodin in the mouse brain. *Synapse* **65**, 763–770.

Cosquer, B., Kuster, N., and Cassel, J. C. (2005). Whole-body exposure to 2.45 GHz electromagnetic fields does not alter 12-arm radial-maze with reduced access to spatial cues in rats. *Behav. Brain Res.* **161**, 331–334.

Eichenbaum, H., Yonelinas, A. P., and Ranganath, C. (2007). The medial temporal lobe and recognition memory. *Annu. Rev. Neurosci.* **30**, 123–152.

Gadek-Michalska, A., Tadeusz, J., Rachwalska, P., and Bugajski, J. (2015). Chronic stress adaptation of the nitric oxide synthases and IL-1β levels in brain structures and hypothalamic-pituitary-adrenal axis activity induced by homotypic stress. *J. Physiol. Pharmacol.* **66**, 427–440.

Gandhi, O. P., Hunt, E. L., and D'Andrea John, A. (1977). Deposition of electromagnetic energy in animals and in models of man with and without grounding and reflector effects. *Radio Sci.* **12**, 39–47.

Garthwaite, J., and Boulton, C. L. (1995). Nitric oxide signaling in the central nervous system. *Annu. Rev. Physiol.* **57**, 683–706.

Gispen, W. H., and Biessels, G.-J. (2000). Cognition and synaptic plasticity in diabetes mellitus. *Trends Neurosci.* **23**, 542–549.

Hongpaisan, J., and Alkon, D. L. (2007). A structural basis for enhancement of long-term associative memory in single dendritic spines regulated by PKC. *Proc. Natl. Acad. Sci U.S.A.* **104**, 19571–19576.

Joëls, M. (2008). Functional actions of corticosteroids in the hippocampus. *Eur. J. Pharmacol.* **583**, 312–321.

Joëls, M., and Baram, T. Z. (2009). The neuro-symphony of stress. *Nat. Rev. Neurosci.* **10**, 459–466.

Kallarackal, A. J., Kvarta, M. D., Cammarata, E., Jaberi, L., Cai, X., Bailey, A. M., and Thompson, S. M. Thompson SM (2013). Chronic stress induces a selective decrease in AMPA receptor-mediated synaptic excitation at hippocampal temporoammonic-CA1 synapses. *J. Neurosci.* **33**, 15669–15674.

Kelleher, R. J. I. I. I., Govindarajan, A., Jung, H. Y., Kang, H., and Tonegawa, S. (2004). Translational control by MAPK signaling in long-term synaptic plasticity and memory. *Cell* **116**, 467–479.

Kolkova, K., Stensman, H., Berezin, V., Bock, E., and Larsson, C. (2005). Distinct roles of PKC isoforms in NCAM-mediated neurite outgrowth. *J. Neurochem.* **92**, 886–894.

Kretz, O., Reichardt, H. M., Schutz, G., and Bock, R. (1999). Corticotropin-releasing hormone expression is the major target for glucocorticoid feedback-control at the hypothalamic level. *Brain Res.* **818**, 488–491.

Lai, H., Horita, A., and Guy, A. (1994). Microwave irradiation affects radial-arm maze performance in the rat. *Bioelectromagnetics* **15**, 95–104.

Li, H. J., Peng, R. Y., Wang, C. Z., Qiao, S. M., Yong, Z., Gao, Y. B., Xu, X. P., Wang, S. X., Dong, J., Zuo, H. Y., *et al.* (2015). Alterations of cognitive function and 5-HT system in rats after long term microwave exposure. *Physiol. Behav.* **140**, 236–246.

Liu, X., Betzenhauser, M. J., Reiken, S., Meli, A. C., Xie, W., Chen, B. X., Arancio, O., and Marks, A. R. (2012). Role of leaky neuronal ryanodine receptors in stress-induced cognitive dysfunction. *Cell* **150**, 1055–1067.

Lynch, M. A. (2004). Long-term potentiation and Memory. *Physiol. Rev.* **84**, 87–136.

Magariños, A. M., and McEwen, B. S. (1995). Stress-induced atrophy of apical dendrites of hippocampal CA3c neurons: Comparison of stressors. *Neuroscience* **69**, 83–88.

McEwen, B. S. (2000). Effects of adverse experiences for brain structure and function. *Biol. Psychiatry* **48**, 721–731.

Neves, G., Cooke, S. F., and Bliss, T. V. P. (2008). Synaptic plasticity, memory and the hippocampus: A neural network approach to causality. *Nat. Rev. Neurosci.* **9**, 65–75.

Nikbakht, N., Zarei, B., Shirani, E., Moshtaghian, J., Esmaeili, A., and Habibian, S. (2012). Experience-dependent expression of rat hippocampal Arc and Homer1a after spatial learning on 8-arm and 12- arm radial mazes. *Neuroscience* **218**, 49–55.

Pavlides, C., Nivon, L. G., and McEwen, B. S. (2002). Effects of chronic stress on hippocampal long-term potentiation. *Hippocampus* **12**, 245–257.

Shahin, S., Banerjee, S., Singh, S. P., and Chaturvedi, C. M. (2015). 2.45 GHz microwave radiation impairs learning and spatial memory via oxidative/nitrosative stress induced p53 dependent/independent hippocampal apoptosis: Molecular basis and underlying mechanism. *Toxicol. Sci.* **148**, 380–399.

Shahin, S., Mishra, V., Singh, S. P., and Chaturvedi, C. M. (2014). 2.45-GHz microwave irradiation adversely affects reproductive function in male mouse, *Mus musculus* by inducing oxidative and nitrosative stress. *Free Radic. Res.* **48**, 511–525.

Shahin, S., Singh, V. P., Shukla, R. K., Dhawan, A., Gangwar, R. K., Singh, S. P., and Chaturvedi, C. M. (2013). 2.45 GHz microwave irradiation induced oxidative stress affects implantation or pregnancy in mice, *Mus musculus*. *Appl. Biochem. Biotechnol.* **169**, 727–1751.

Shirai, Y., Adachi, N., and Saito, N. (2008). Protein kinase Cepsilon: Function in neurons. *Febs J.* **275**, 3988–3994.

Sousa, N., and Almeida, O. F. (2002). Corticosteroids: sculptors of the hippocampal formation. *Rev. Neurosci.* **13**, 59–84.

Sousa, N., Lukoyanov, N. V., Madeira, M. D., Almeida, O. F., and Paula-Barbosa, M. M. (2000). Reorganization of the morphology of hippocampal neurites and synapses after stress-induced damage correlates with behavioral improvement. *Neuroscience* **97**, 253–266.

Sugama, S., Takenouchi, T., Fujita, M., Kitani, H., Conti, B., and Hashimoto, M. (2013). Corticosteroids limit microglial activation occurring during acute stress. *Neuroscience* **232**, 13–20.

Sun, M.-K., Hongpaisan, J., Nelson, T. J., and Alkon, D. L. (2008). Post stroke neuronal rescue and synaptogenesis mediated in vivo by protein kinase C in adult brains. *Proc. Natl. Acad. Sci. U.S.A.* **105**, 13620–13625.

Tochio, H., Mok, Y. K., Zhang, Q., Kan, H. M., Bredt, D. S., and Zhang, M. (2000). Formation of nNOS/PSD-95 PDZ dimer requires a preformed β-finger structure from the nNOS PDZ domain. *J. Mol. Biol.* **303**, 359–370.

Tran, E. H., Hardin-Pouzet, H., Verge, G., and Owens, T. (1997). Astrocytes and microglia express inducible nitric oxide synthase in mice with experimental allergic encephalomyelitis. *J. Neuroimmunol.* **74**, 121–129.

Vyas, A., Mitra, R., Shankaranarayana Rao, B. S., and Chattarji, S. (2002). Chronic stress induces contrasting patterns of dendritic remodeling in hippocampal and amygdaloid neurons. *J. Neurosci.* **22**, 6810–6818.

Wang, B., and Lai, H. (2000). Acute exposure to pulsed 2.450-MHz microwaves affects water-maze performance of rats. *Bioelectromagnetics* **21**, 52–56.

Wang, H., Peng, R., Zhao, L., Wang, S., Gao, Y., Wang, L., Zuo, H., Dong, J., Xu, X., Zhou, H., *et al.* (2015). The relationship between NMDA receptors and microwave-induced learning and memory impairment: A long-term observation on Wistar rats. *Int. J. Radiat. Biol.* **91**, 262–269.

Xiong, L., Sun, C. F., Zhang, J., Gao, Y. B., Wang, L. F., Zuo, H. Y., Wang, S. M., Zhou, H. M., Xu, X. P., Dong, J., *et al.* (2015). Microwave exposure impairs synaptic plasticity in the rat hippocampus and PC12 cells through over-activation of the NMDA receptor signaling pathway. *Biomed. Environ. Sci.* **28**, 13–24.

Yakymenko, I., Tsybulin, O., Sidorik, E., Henshel, D., Kyrylenko, O., and Kyrylenko, S. (2016). Oxidative mechanisms of biological activity of low-intensity radiofrequency radiation. *Electromagn. Biol. Med.* **35**, 186–202.

Zuo, H., Lin, T., Wang, D., Peng, R., Wang, S., Gao, Y., Xu, X., Zhao, L., Wang, S., and Su, Z. (2015). RKIP regulates neural cell apoptosis induced by exposure to microwave radiation partly through the MEK/ERK/CREB pathway. *Mol. Neurobiol.* **51**, 1520–1529.